

**ELECTRICAL ENERGY SAVING IN AIR CONDITIONER
BY PHOTOVOLTAIC MODULE ASSISTED WITH PHASE
CHANGE MATERIAL**



SONGHENG LOEM

**MASTER OF ENGINEERING
IN ENERGY ENGINEERING**

ลิขสิทธิ์มหาวิทยาลัยเชียงใหม่
Copyright© by Chiang Mai University
All rights reserved

**GRADUATE SCHOOL
CHIANG MAI UNIVERSITY
JUNE 2019**

**ELECTRICAL ENERGY SAVING IN AIR CONDITIONER BY
PHOTOVOLTAIC MODULE ASSISTED WITH PHASE
CHANGE MATERIAL**

SONGHENG LOEM

**A THESIS SUBMITTED TO CHIANG MAI UNIVERSITY IN PARTIAL
FULFILLMENT OF THE REQUIREMENTS FOR THE DEGREE OF
MASTER OF ENGINEERING
IN ENERGY ENGINEERING**

**ลิขสิทธิ์มหาวิทยาลัยเชียงใหม่
Copyright© by Chiang Mai University
All rights reserved**

GRADUATE SCHOOL, CHIANG MAI UNIVERSITY

JUNE 2019

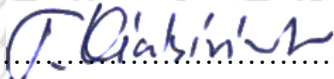
**ELECTRICAL ENERGY SAVING IN AIR CONDITIONER BY
PHOTOVOLTAIC MODULE ASSISTED WITH PHASE
CHANGE MATERIAL**

SONGHENG LOEM

THIS THESIS HAS BEEN APPROVED TO BE A PARTIAL FULFILLMENT OF
THE REQUIREMENTS FOR THE DEGREE OF
MASTER OF ENGINEERING
IN ENERGY ENGINEERING

Examination Committee:

Advisor:

 Chairperson 
(Dr. Atipoang Nuntaphan) (Prof. Dr. Tanongkiat Kiatsiriroat)

 Member
(Prof. Dr. Tanongkiat Kiatsiriroat)

 Member
(Asst. Prof. Dr. Attakorn Asanakham)

 Member
(Dr. Thoranis Deethayat)

19 June 2019

Copyright © by Chiang Mai University

ACKNOWLEDGEMENT

Foremost, I would like to express my sincere gratitude to my advisor, Prof. Dr. Tanongkiat Kiatsiriroat for the continuous support of my master study and research, for his patience, motivation, enthusiasm, and immense knowledge. His guidance helped me in all the time of research and writing of this thesis. I could not have imagined having a better advisor and mentor for my master study.

Besides my adviser, I would love to thank the rest of my thesis committee: Asst. Prof. Dr. Attakorn Asanakham, Dr. Thoranis Deethayat, and Dr. Atipoang Nuntaphan, insightful judgments, and hard questions.

My truthful thanks also go to Faculty of Engineering (Research Assistant Program); Center of Excellence for Renewable Energy, Chiang Mai University; and National Research Council of Thailand through the project on “Development of Alternative Energy Prototypes for Green Communities” for supporting testing facilities and financing support.

I further wish to express my gratitude to all seniors and staffs of the laboratory of thermal system research unit for their support, assistance, guidance, and friendships.

Finally, I would like to give my thanks to my parents for almost unbelievable care. They are the most important people in my life, and I dedicate this thesis to them.

ลิขสิทธิ์มหาวิทยาลัยเชียงใหม่
Copyright© by Chiang Mai University
All rights reserved

Songheng Loem

หัวข้อวิทยานิพนธ์	การลดการใช้พลังงานไฟฟ้าในเครื่องปรับอากาศโดยโมดูลโฟโตวอลเทอิกเสริมด้วยสารเปลี่ยนสถานะ
ผู้เขียน	นายสงheng ลิม
ปริญญา	วิศวกรรมศาสตรมหาบัณฑิต(วิศวกรรมพลังงาน)
อาจารย์ที่ปรึกษา	ศาสตราจารย์ ดร.ทงเกียรติ เกียรติศิริโรจน์

บทคัดย่อ

ในงานวิจัยนี้ได้ศึกษาการลดการใช้ไฟฟ้าจากสายส่งของการทำความเย็นที่มีอินเวอร์เตอร์ โดยใช้สารเปลี่ยนสถานะ RH-18HC แบบแผ่นเบดเป็นตัวเก็บสะสมความเย็นแผ่นเบดสารเปลี่ยนสถานะ (พีซีเอ็ม) ,RH-18HCซึ่งมีอุณหภูมิจุดหลอมเหลวประมาณ 18°C ถูกใช้เป็นตัวสะสมความเย็นสำหรับคอยล์อีวาपोเรเตอร์ การทำงานของสารเปลี่ยนสถานะมี 2 ช่วงเวลา ช่วงประจุ , เบดพีซีเอ็มจะถูกประจุด้วยอากาศเย็นจากคอยล์อีวาपोเรเตอร์ในช่วงเช้าซึ่งมีอุณหภูมิอากาศค่อนข้างต่ำ ; การคายประจุ , ซึ่งอากาศก่อนเข้าคอยล์เย็นจะผ่านเบดซึ่งผ่านการประจุแล้ว ทำให้อากาศจะมีอุณหภูมิต่ำลงก่อนเข้าคอยล์อีวาपोเรเตอร์ซึ่งจะช่วยลดภาระทางความร้อนที่คอยล์อีวาपोเรเตอร์ ส่งผลให้ความต้องการกำลังไฟฟ้าที่คอมเพรสเซอร์ลดลง จากผลการศึกษาพบว่า เมื่อใช้เบดหนา 0.24 m สามารถลดการใช้ไฟฟ้าจากสายส่งได้ 13.84% และ 16.13% ในฤดูหนาวและฤดูร้อนที่จังหวัดเชียงใหม่

นอกจากนี้ ยังมีการใช้โมดูลโฟโตวอลเทอิก (PV module) ชนิดโพลีคริสตัลไลน์ ขนาด 0.99 m x 1.96 m กำลังการผลิตไฟฟ้าแต่ละโมดูล 320 W ภายใต้การทดสอบที่เงื่อนไขมาตรฐาน แต่ละโมดูลเอียงทำมุม 18°47' หันหน้าไปทางทิศใต้ สำหรับสภาวะภูมิอากาศเชียงใหม่ โมดูลพีวีจะต่อตรงเข้ากับเครื่องทำความเย็นและจะมีไฟฟ้าจากสายส่งเสริมกรณีความเข้มรังสีอาทิตย์ไม่เพียงพอ จำนวนโมดูลที่เหมาะสม จะพิจารณาจากมูลค่าปัจจุบันของค่าใช้จ่ายประกอบด้วยเงินลงทุน ค่าไฟฟ้าจากสายส่ง ค่าดูแลรักษา และมูลค่าซาก โดยคิดอัตราส่วน 6.25% ตลอดอายุการทำงาน 25 ปี โดยคิดค่าไฟฟ้าต่อหน่วยที่ 5.78 baht/kWh ซึ่งจะได้จำนวนโมดูลที่เหมาะสมที่ 3 โมดูล และมีระยะเวลาคืนทุน 8.92 ปี

Thesis Title Electrical Energy Saving in Air Conditioner by Photovoltaic Module Assisted with Phase Change Material

Author Mr. Songheng Loem

Degree Master of Engineering (Energy Engineering)

Advisor Prof. Dr. Tanongkiat Kiatsirirot

ABSTRACT

This study attempts to find out the electrical energy reduction from grid line for an inverter air conditioning unit using the solar energy as well as the energy cool storage. A packed bed of phase change material (PCM) RT-18 HC, having melting point around 18 °C was considered as the energy cool storage for a 1 TR R-410a air conditioner unit. The PCM packed bed operation was divided into 2 periods: charging period, the PCM bed was fully charged by supplying the cool air from evaporator coil in the early morning with low ambient temperature; discharging period, the air before entering the evaporator coil was passing through the PCM bed then the cooling load at the evaporator was reduced and also the required electrical power at the compressor with the bed thickness of 0.24 m, the electrical power saving from the grid line were 13.84% and 16.13% in winter and summer, respectively. On the other hand, the polycrystalline PV modules having a size of 0.99 m x 1.96 m with a maximum electrical power output of 320 W under standard test condition were integrated to the tested system. The modules installed with the tilt angle of 18°47' and south facing for Chiang Mai condition. The PV modules were directly connected to the inverter air conditioner. The electrical grid was supplied to the air conditioner unit when the solar radiation was insufficient.

The optimum number of PV module could be determined at the lowest present worth of the total investment cost, the electricity cost from the grid line, the maintenance cost and the salvage value with 6.25% annual discount rate for 25 years of service. The unit cost

of grid electricity was 5.78 baht/kWh. It could be found that the optimum number of PV modules at the lowest total expenses for the air conditioner unit with assisted PCM bed was 3 modules with the payback period 8.92 years.



ลิขสิทธิ์มหาวิทยาลัยเชียงใหม่
Copyright© by Chiang Mai University
All rights reserved

CONTENTS

	Page
ACKNOWLEDGEMENT	c
ABSTRACT IN THAI	d
ABSTRACT IN ENGLISH	e
CONTENTS	g
LIST OF TABLES	j
LIST OF FIGURES	k
LIST OF ABBREVIATIONS	n
LIST OF SYMBOLS	o
CHAPTER 1 Introduction	1
1.1 Background and Problem Statement	1
1.2 Literature Review	2
1.3 Objectives of the Research	9
1.4 Scope of the Research	9
1.5 Benefits of the Research	9
CHAPTER 2 Theory	10
2.1 Energy Consumption of an Inverter Air Conditioner Unit	10
2.2 Energy Consumption of an Inverter Air conditioner Unit with Assisted PCM Packed Bed Cool Storage	12
2.3 Mathematical Model of PCM Packed Bed Cool Storage	12
2.4 Electrical Power Equation of PV Module	16
2.5 Economic Analysis	18
CHAPTER 3 Experimental Set-Up	19
3.1 Experimental Construction	19
3.2 Conventional Inverter Air Conditioner Unit	20

3.3 PCM Packed Bed Cool Storage	22
3.4 Solar PV Connected Grid Line	24
3.5 Experimental Components	25
3.6 Measuring Instrument	29
CHAPTER 4 Thermal Characteristics on Charging and Discharging of RT-18 HC PCM Packed Bed Cool Storage	33
4.1 Charging Period	33
4.2 Discharging Period	36
CHAPTER 5 Air Conditioner Unit with and without Assisted PCM Packed Bed Cool Storage	39
5.1 Thermal Performance of the Conventional Air Conditioner Unit	39
5.2 The Effect of PCM Bed Cool Storage on the Inverter Air Conditioner Operation	41
CHAPTER 6 PV Module Generation for Inverter Air conditioner Unit	45
6.1 Validation of PV Power Generation and Module Temperature	45
6.2 Electrical Power Generation of PV Module	46
CHAPTER 7 Energy Saving of the PV-Air Conditioner Unit with Assisted PCM bed Cool Storage	49
7.1 PV Modules Power Generation for the Air Conditioner with Assisted PCM Bed Cool Storage	49
7.2 Long Term Analysis of the PV-Air Conditioner Unit with Assisted PCM Bed Cool Storage	50
CHAPTER 8 Conclusions	52
REFERENCES	53
APPENDICES	56
APPENDIX A	57
APPENDIX B	61
APPENDIX C	65
APPENDIX D	67



ลิขสิทธิ์มหาวิทยาลัยเชียงใหม่
Copyright© by Chiang Mai University
All rights reserved

LIST OF TABLES

	Page
Table 1.1 Optimum module numbers of the solar modules.	3
Table 1.2 Description of PCM slabs [8].	5
Table 2.1 The maximum and the minimum ambient temperatures of Chiang Mai, Thailand [17].	17
Table 3.1 Descriptions of the inverter air conditioner R-410a.	26
Table 3.2 Specification of PV module.	28
Table 3.3 Descriptions of the RT-18HC.	29
Table 3.4 Measurement rang and accuracy of instruments.	30
Table 5.1 Energy consumption of the air conditioner unit with and without assisted PCM bed cool storage.	44

LIST OF FIGURES

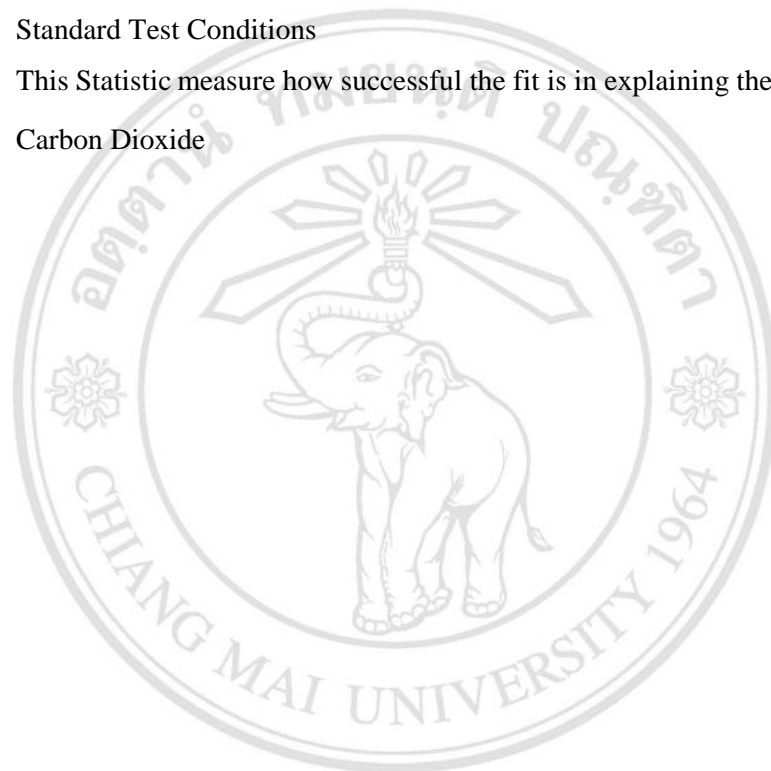
	Page
Figure 1.1 State of PCM in solidification and melting.	2
Figure 1.2 Solar air conditioning system [5].	3
Figure 1.3 Schematic diagram of the air conditioner integrated with PCM thermal storage [7].	4
Figure 1.4 Schematic sketch of the air cooling system incorporating with LHTS [8].	5
Figure 1.5 Diagrams of HVAC system for simulations [9].	6
Figure 1.6 Cylindrical storage filled with spherically encapsulated PCM [10-12].	6
Figure 1.7 PCM storage for free cooling of buildings:(a) daytime operation and (b) nighttime operation [11].	7
Figure 1.8 Schematic of the testing room. (a)The modified system, (b) Charging operation and(c) Discharging operation [13].	7
Figure 2.1 Thermal performance of inverter air conditioner.	10
Figure 2.2 Energy balance of evaporator.	11
Figure 2.3 PCM packed bed storage.	12
Figure 2.4 Enthalpy with a various temperature of PCM in each phase change.	14
Figure 2.5 Flowchart of the simulation program for evaluating the PCM bed temperature and the air leaving PCM bed temperature for charging and discharging periods.	16
Figure 3.1 Schematic sketch of the modified air conditioner unit in the present study.	20
Figure 3.2 Schematic sketch of the conventional air conditioner unit.	20
Figure 3.3 Measurement points of a conventional air conditioner.	21
Figure 3.4 Humidity controller.	21
Figure 3.5 Electrical heater.	22
Figure 3.6 Integration of the PCM packed bed and the evaporator coil.	22
Figure 3.7 Charging period of the PCM packed bed and measurement temperature points of the air and PCM packed bed.	23

Figure 3.8 Discharging period of the PCM packed bed and measurement temperature points of the air and PCM packed bed.	24
Figure 3.9 On-grid solar PV powered the air conditioner.	25
Figure 3.10 Schematic diagram of measurement points.	25
Figure 3.11 Basic of air conditioning cycle.	26
Figure 3.12 Schematic diagram of solar cell [17].	27
Figure 3.13 Series of a PV modules for the unit.	27
Figure 3.14 Store and release of phase change material cycle [18].	28
Figure 3.15 Measuring instruments.	30
Figure 3.16 Flowchart of the study process.	31
Figure 4.1 Variation of bed temperature with time at various bed thicknesses during charging period.	34
Figure 4.2 Variation of outlet air temperature with time at various thicknesses during charging period.	34
Figure 4.3 Effect of mass flow rates on PCM charging period.	35
Figure 4.4 Dimensionless terms, θ , τ and Y (charging period).	35
Figure 4.5 Variation of bed temperature with time at various bed thicknesses during discharging period.	36
Figure 4.6 Variation of outlet air temperature with time at various thicknesses during	37
Figure 4.7 Effect of mass flow rates on PCM discharging period.	37
Figure 4.8 Dimensionless terms, θ , τ and Y (discharging period).	38
Figure 4.9 Experimental results of the inlet air temperature at the evaporator coil with and without PCM bed.	38
Figure 5.1 Thermal performance of the conventional inverter air conditioner unit.	40
Figure 5.2 Electrical power of conventional inverter air conditioner unit in summer.	40
Figure 5.3 Electrical power of conventional inverter air conditioner unit in winter.	41
Figure 5.4 The room temperature and the surrounding ambient temperature during the tested work.	41
Figure 5.5 Experimental results of the conventional air conditioner unit with and without assisted PCM bed. (a) 0.08m. (b) 0.24m.	43

Figure 6.1 Ambient temperature and solar radiation on clear sky day.	45
Figure 6.2 Validation of module temperature and PV power output.	46
Figure 6.3 Electrical power reduction from grid line by four PV modules to air conditioner unit. (a) clear sky day. (b) cloudy day. (c) mostly cloudy day.	47
Figure 6.4 Electrical power reduction from grid line by four PV modules to the air conditioner unit. (a) a day in winter. (b) a day in summer.	48
Figure 7.1 Electrical power reduction from grid line by four PV modules to air conditioner unit with assisted PCM bed. (a) a day in winter. (b) a day in summer.	50
Figure 7.2 Optimum number of the PV-air conditioner with assisted PCM bed.	51
Figure 7.3 Payback period of the PV-air conditioner with assisted PCM bed.	51

LIST OF ABBREVIATIONS

PV	Photovoltaic
PCM	Phase Change Material
SEER	Seasonal Energy Efficiency Ratio
NOCT	Normal operating cell temperature
STC	Standard Test Conditions
R-square	This Statistic measure how successful the fit is in explaining the variation of the data
CO ₂	Carbon Dioxide



ลิขสิทธิ์มหาวิทยาลัยเชียงใหม่
Copyright© by Chiang Mai University
All rights reserved

LIST OF SYMBOLS

Nomenclature

Q	Cooling load capacity (kW)
P	Power (kW)
h	Enthalpy (kJ/kg)
\dot{m}	Mass flow rate (kg/s)
T	Temperature ($^{\circ}\text{C}$)
ω_1	Inlet humidity ratio (kg/kg)
ω_2	Outlet humidity ratio (kg/kg)
L	Packed bed length (m)
X	Packed bed thickness (m)
x	Position at any section of the packed bed
A	Cross-sectional area (m^2)
V	Volume (m^3)
M	Mass (kg)
D	Diameter (m)
C_p	Specific heat capacity (kJ/kg $^{\circ}\text{C}$)
h_v	Volumetric heat transfer coefficient ($\text{W}/\text{m}^3 \text{ }^{\circ}\text{C}$)
G	Mass flow rate per area (kg/s m^2)
t	Time (s)
l	PCM latent heat (kJ/kg)
N	Section
Y	Dimensionless of thickness and mass flow rate
Sim	Simulation
Exp	Experiment
I_T	Solar radiation intensity on tilt plane (W/m^2)
I_b	Beam radiation on a horizontal surface (W/m^2)
I_d	Diffuse radiation on a horizontal surface (W/m^2)
R_b	Ratio of beam radiation on a tilted surface to that on a horizontal surface
ρ_g	Ground reflectance
C	Cost

Subscripts

<i>AC</i>	Air conditioner
<i>PV</i>	Photovoltaic
<i>Eva</i>	Evaporator coil
<i>Cond</i>	Condenser
<i>a</i>	Air
<i>db</i>	Dry bulb
<i>wb</i>	Wet bulb
<i>r</i>	Room
<i>amb</i>	Ambient
<i>w</i>	Water
<i>b</i>	Bed
<i>l</i>	Liquide
<i>m</i>	Melting
<i>s</i>	Solid
<i>i and i + 1</i>	The entering and the exit of the i^{th} section
<i>inlet</i>	Inlet condition
<i>ref</i>	Reference at initial condition
<i>max</i>	Maximum
<i>min</i>	Minimum
<i>C</i>	Cell
<i>STC</i>	Standard Test Conditions
β	tilt angle ($^{\circ}$)
ε	Void fraction
ρ	Density (kg/m^3)
τ	Dimensionless of time
θ	Dimensionless of temperature
Δ	Increment
γ	Temperature coefficient of power ($^{\circ}\text{C}^{-1}$)
<i>inv</i>	Investment
<i>O&m</i>	Operation and maintenance
<i>sv</i>	Salvage value

CHAPTER 1

Introduction

This chapter gave the energy demand of the air conditioner in building air conditioner application as well as the literature review of solar power energy in reducing of electrical grid and energy cool storage of phase change material for improving the energy efficiency of air conditioner.

1.1 Background and Problem Statement

Air conditioning system in building is considered as the large proportion of energy consumption. Percentage of electrical energy consumed for air conditioning in household or office building uses was 50%-70% [1,2]. Not only energy cost but also high CO₂ emission due to power generation is obtained. To alternate the problem, PV module is an effective way to reduce electrical energy from the grid line in view of the consumption of PV module raises as the growing demand for sustainable energy. Thus, CO₂ could also be reduced. Another approval is to use phase change material (PCM) as cool storage to integrate with the air conditioner. With a good management, the PCM could store coolness with a large amount of heat storage capacity during the off-peak cooling load and generate cooling air using its latent heat to reduce air temperature before entering the evaporator coil during the on-peak cooling load as shown in Figure 1.1. Then the power consumption for a whole day could be reduced. In this study, a use of PV module to generate electrical power to an air conditioner with a thermal management by taking PCM to hold coolness in the off-peak and generate cool air in the on-peak will be considered. Investigation on the sizing of the PV module and the PCM amount to reduce on-grid power consumption in the air conditioner will be carried out.

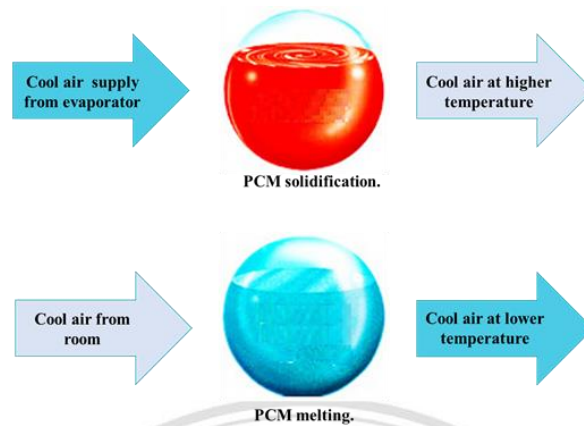


Figure 1.1 State of PCM in solidification and melting [3].

1.2 Literature Review

In this paper, the literature review is divided into two parts. The first one is solar air-conditioning system and the other one is phase change material (PCM) energy storage for cooling.

1.2.1 Solar air conditioning system

The study of the development or evaluation of the technology of the enhanced grid-connected photovoltaic solar air conditioning were conducted by many authors as follows.

F. J. Aguilera et al [4] analyzed the possibility of using photovoltaic panels to produce electricity that was used to power the compressor of an inverter air conditioning/heat pump unit; without batteries storage or any inverter regulators. The aim of the project was to study an "inverter" heat pump with a nominal cooling capacity of 3.52 kW and a nominal heating capacity of 3.81 kW. The "inverter module" got the electricity from the grid and three 235 Wp photovoltaic panels simultaneously. The experimental results showed that during summer and winter, the solar contributions of PV panels were about 65% and 50% of total energy requirements, respectively.

D. Parker and J. Dunlop [5] used photovoltaic (PV) module for residential air conditioning. The grid power for the cooling load could be decreased by over 75%.

K. S. Al Qdah [6] focused on design and construction of solar-powered air conditioning system operating under AlMadinah AlMunawwarah climatic condition in Saudi Arabia as shown in Figure 1.2. The outside temperature was almost higher than 42 °C in

summer. The results showed that several characteristics that must be given such as the PV module and the air conditioner performances to evaluate the electrical power for running the air conditioner. A suitable number of the solar panels each of 310W output was 6 modules, based on 1-ton refrigeration cooling load.



Figure 1.2 Solar air conditioning system [6].

S. Loem and T. Deethayat [7] simulated electrical energy generated by a set of solar cell modules with and without 5 mm thickness RT-42 phase change material (PCM) cooling at the back of the module to match with a 2 tons air conditioning load. The optimum module numbers under Chiang Mai climate were evaluated as given in Table 1.1.

Table 1.1 Optimum module numbers of the solar modules.

	PV	PV-PCM
Optimum number of solar cell module	6	4
Annual electrical energy demand from the grid line(kWh)	1014.92	1267.51
The payback period (year)	7.7	8.7

From Table 1.1, even the payback period of the PV-PCM was longer due to a high price of the PCM but if the price was 30.56% reduction the unit could be competitive. It could be noted that the number of the solar cell module could be reduced compared with the normal PV module.

1.2.2 Phase change material (PCM) cool energy storage

In the office building, the main electrical energy consumption devoted to air conditioning system. Thus, it is crucial to find a method that could be used to reduce the electricity consumption of the machine or to intensify its performance. Some

researchers have achieved with the phase change material (PCM) as a cold storage to reduce a load usage as presented in literature review below.

D. Zhao and G. Tan [8] studied a shell-and-tube based phase change material (PCM) thermal storage system with conventional air conditioner to increase cooling coefficient of performance (COP). The proposed PCM thermal storage unit used two kinds of heat transfer fluids. Water was used for charging loop while air was used for discharging loop. A schematic diagram of the air conditioner integrated with the PCM thermal storage was shown in Figure 1.3.

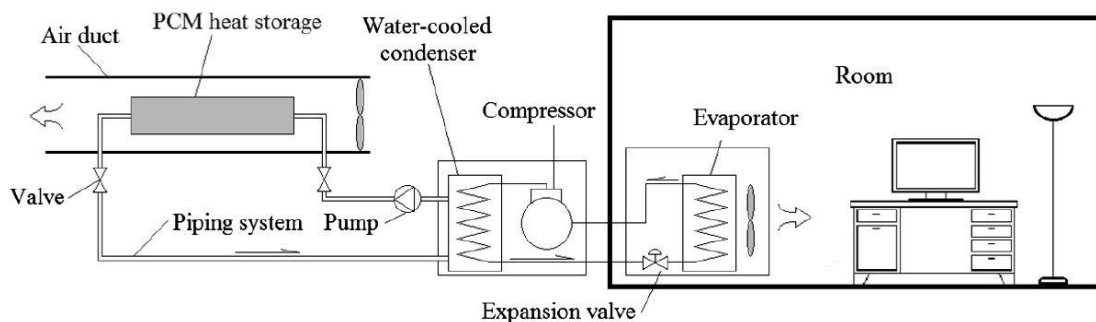


Figure 1.3 Schematic diagram of the air conditioner integrated with PCM thermal storage [8].

Numerical model for the PCM thermal storage system was evaluated with the effects of fluids inlet temperatures, mass flow rate and conductive fin height. The model was designed according to the cooling load profile and achieved the best performance of the PCM thermal storage system. The results showed that the proposed PCM thermal storage system could replace a conventional cooling tower for water-cooling at the air conditioner condenser and the new design gave about 25.6% increase in the COP.

A. H. Mosaffa and L. Garousi Farshi [9] presented an air conditioning system combined with a set of PCM slabs as a latent heat thermal storage unit (LHTS). This study analyzed three cases with different PCM slab sizes and different PCM types. Description of all PCM was presented in Table 1.2.

Table 1.2 Description of PCM slabs [9].

Case no.	Length, l	Thickness, d	PCM
case 1	1.8 m	15 mm	RT27
case 2	1.7 m	10 mm	S27
case 3	1.4 m	15 mm	SP25

The analysis was conducted from exergoeconomic and environmental points of view. Figure 1.4 showed the schematic sketch of the proposed air conditioning system incorporating with a LHTS unit. During the off-peak hours (nighttime), the heat was released from the PCM by employing a conventional vapor compression refrigeration system when the electricity service was inexpensive. Then the solidified PCM was used for air cooling during the hot hours of day. The analysis resulted that: (1) RT27 gave the highest value of exergy efficiency, (2) S27 showed the lowest value of total cost rate and (3) SP25 presented the highest value of the coefficient of performance.

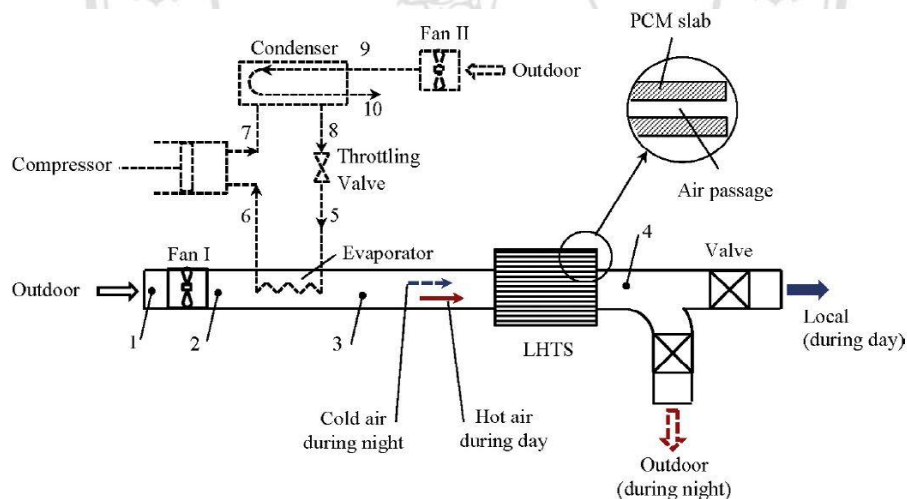


Figure 1.4 Schematic sketch of the air cooling system incorporating with LHTS [9].

M. Yamaha and S. Misaki [10] proposed an air distribution system with PCMs in air ducts for peak air-conditioning load shaving. The concept was shown in Figure 1.5. The PCM storage was charged from 5:00 am to 8:00 am (the charging mode) by the air flowing in the closed loop of the PCM storage tank and the air conditioner was used to solidify the storage medium. When the charging operation finished, the ordinary air conditioning operation started, in which the air was bypassed the PCM storage tank and fed into the occupied room. The discharging operation was occurred from 13:00 pm to

16:00 pm. At this mode, the outdoor air temperature was slightly higher than that of the PCM melting point thus it could be used to flow through the PCM tank and to the room.

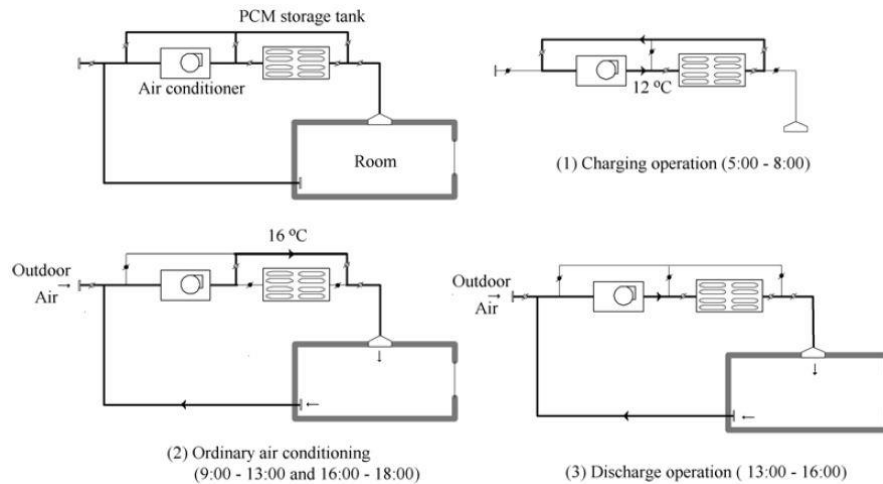


Figure 1.5 Diagrams of HVAC system for simulations [10].

The simulation study based on a part of one floor of an office building in Japan showed that the use of 400 kg MT-19 PCM for a room with an area of 73.8 m² could maintain a constant indoor temperature without using any cold source in a hot summer day.

C. Arkar et al [11-13] studied cylindrical thermal energy storage unit filled with spherically encapsulated PCM (RT-20) shown in Figure 1.6.

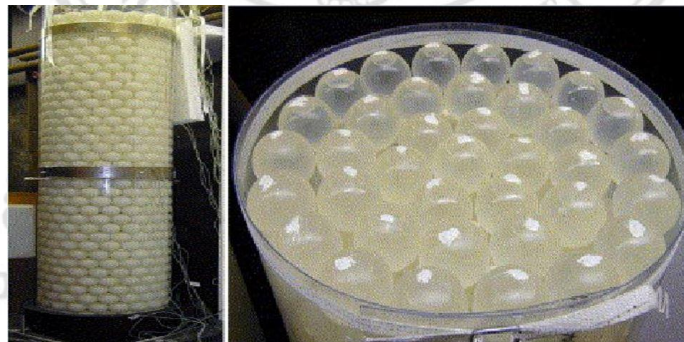


Figure 1.6 Cylindrical storage filled with spherically encapsulated PCM [11-13].

The storage was installed in a building room for studying free cooling as shown in Figure 1.7. Mechanical ventilation system was integrated with latent heat thermal energy storage (LHTES). During the nighttime, the ambient temperature was lower than the temperature inside the room then the ambient air was ventilated and flowing through the LHTES to accumulate the coolness. A high room temperature occurred around noon then the outside air was used to pass the LHTES inside the room for reducing the air

temperature. The study concluded that about 6.4 kg of PCM per m² of floor area with air flow rate of 1.0–1.5 m³.h⁻¹ per kg of PCM was optimum to ensure maximum cooling degree hours.

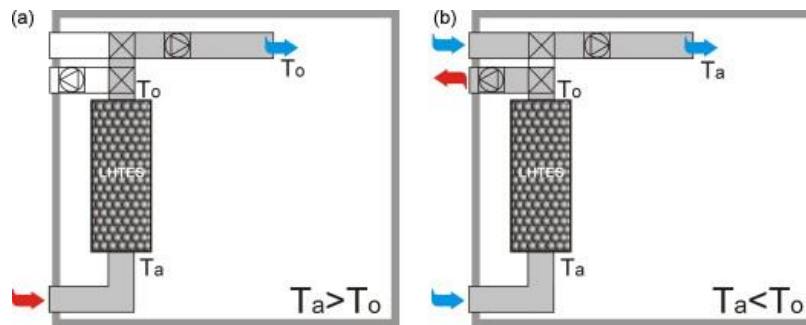


Figure 1.7 PCM storage for free cooling of buildings:(a) daytime operation and (b) nighttime operation [12].

N. Chaiyat and T. Kiatsiriroat [14] used RT-20 PCM packed bed contained in a set of celluloid balls. The melting point of the PCM was about 20 °C. The PCM bed was taken as a cool storage for a 2 TR air conditioner. The packed PCM bed thickness was 40cm. The solidified RT-20 PCM could maintain the return air temperature before entering the evaporator of the air conditioner to be about 20 °C for 3 hours thus the electrical energy consumption to run the air conditioner could be less than that of the normal system. The result showed that the electrical power of the modified system could be saved around 9%. The schematic sketches of the experimental study were shown in Figure 1.8.

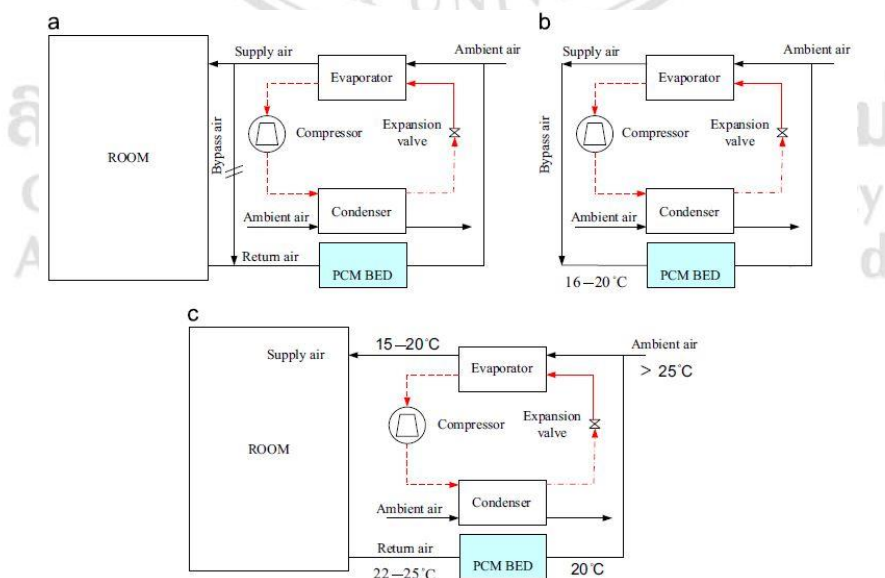
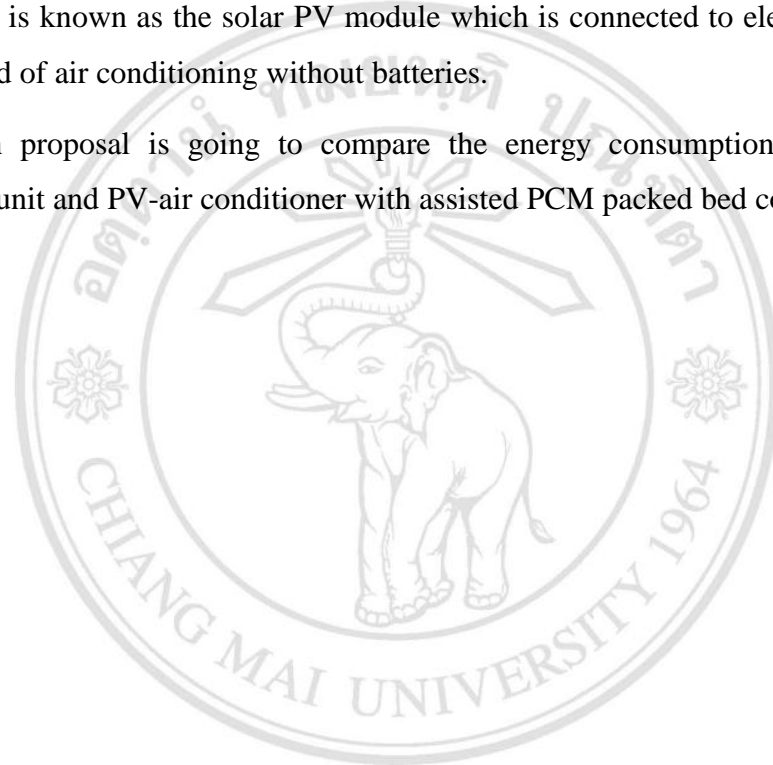


Figure 1.8 Schematic of the testing room. (a)The modified system, (b) Charging operation and(c) Discharging operation [14].

In the present study, similar to M. Yamaha and S. Misaki [10] and N. Chaiyat and T. Kiatsiriroat [14], a well-insulated packed bed containing PCM balls each is 40mm in diameter and encapsulated the paraffin wax having melting point around 18°C will be integrated with an air conditioner evaporator coil inside a testing room. Numerical method will be used to evaluate the thickness of the packed bed at a given of charging and discharging periods. The experimental work is performed in a testing room with cooling load around 1 ton of refrigeration (TR). In this operation, the on-grid solar power system is known as the solar PV module which is connected to electrical grid to power the load of air conditioning without batteries.

This research proposal is going to compare the energy consumption between the conventional unit and PV-air conditioner with assisted PCM packed bed cool storage.



ลิขสิทธิ์มหาวิทยาลัยเชียงใหม่
Copyright© by Chiang Mai University
All rights reserved

1.3 Objectives of the Research

- 1.3.1 To study the phenomena of charging and discharging behaviors of the PCM packed bed.
- 1.3.2 To find the appropriate PCM packed bed thickness in the reduction of electrical power of the air conditioner.
- 1.3.3 To find out the size of the PV module for running the air conditioner with assisted PCM bed and examine the grid line electrical energy saving.

1.4 Scope of the Research

- 1.4.1 The experiment is done at the Thermal System Research Unit Laboratory under the climate of Chiang Mai with latitude 18°47' North.
- 1.4.2 The inverter air conditioner having a cooling load around 1 ton of refrigeration (TR).
- 1.4.3 Electrical heater having capacity around 1.5kW and humidity controller is used in this experimental work.
- 1.4.4 Polycrystalline solar cells having maximum power output 320Wp/module.
- 1.4.5 Phase change material PCM RT-18 HC having melting point around 18 °C is applied with the air conditioner.

1.5 Benefits of the Research

- 1.5.1 The PV module and the phase change material (PCM) could reduce a large amount of electrical power from grid line.
- 1.5.2 The renewable energy is not only reduced electrical power from the grid line, but it also helps to reduce the CO₂ as well

CHAPTER 2

Theory

This chapter provided the equation of the seasonal energy efficiency ratio (SEER) and the output power of solar photovoltaic of the air conditioner. The numerical enthalpy method was also developed to predict the bed temperature and the outlet air temperature of the PCM packed bed.

2.1 Energy Consumption of an Inverter Air Conditioner Unit

The seasonal energy efficiency ratio (SEER) of the air conditioner is the ratio of the cooling capacity Q_{AC} (kWh) to the power input of the unit P_{AC} (kWh) (more efficient - the higher SEER). SEER is also used for the estimation of energy efficiency of air conditioners due to an inverter compressor of the air conditioner runs at variable speeds based on the ambient temperature. The outdoor temperature affected to the seasonal energy efficiency ratio as shown in Figure 2.1.

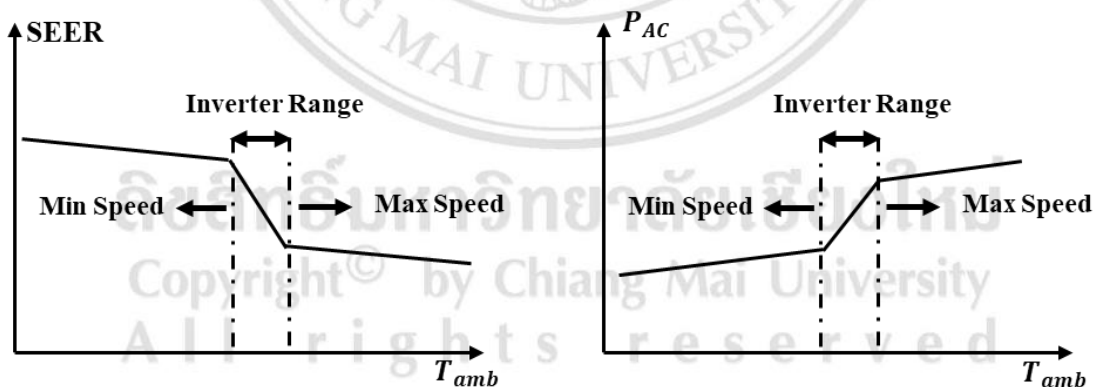


Figure 2.1 Thermal performance of inverter air conditioner.

The energy efficiency ratio could be calculated by

$$SEER = \frac{Q_{AC}}{P_{AC}} \quad (2.1)$$

To know the total heat removed by the evaporator, wet bulb temperature T_{wb} ($^{\circ}C$) and dry bulb temperature T_{db} ($^{\circ}C$) before and leaving evaporator of an air conditioning unit

will be used to find the enthalpy $(\Delta h)_a$ (kJ) at a specific time and the energy loss through condensing water. The air mass flow rate \dot{m}_a (kg/s) flowing through the evaporator coil is considered. Therefore, the energy balance of evaporator could be shown as follows,

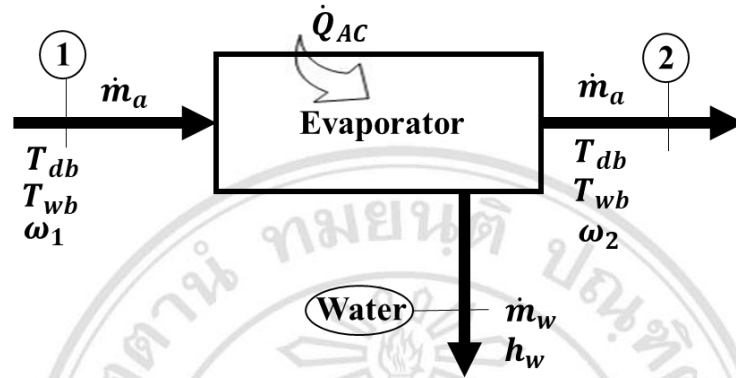


Figure 2.2 Energy balance of evaporator.

The heat generated can be formed as below,

$$\dot{Q}_{AC} = \dot{m}_a(\Delta h)_a - \dot{m}_w h_w \quad (2.2)$$

$$\dot{Q}_{AC} = \dot{m}_a(h_1 - h_2)_a - \dot{m}_a(\omega_1 - \omega_2)h_w \quad (2.3)$$

Thus, the three equation of *SEER* equations could be formed as follows,

Minimum speed of inverter compressor

$$SEER = a_1(T_{amb}) + b_1 \quad (2.4)$$

Inverter operation range

$$SEER = a_2(T_{amb}) + b_2 \quad (2.5)$$

Maximum speed of inverter compressor

$$SEER = a_3(T_{amb}) + b_3 \quad (2.6)$$

Where $a_1, a_2, a_3, b_1, b_2,$ and b_3 are the coefficients of the equations, T_{amb} is the ambient temperature ($^{\circ}\text{C}$), \dot{m}_w is the mass flow rate of condensing water (kg/s), h_w is the enthalpy of water (kJ), and ω_1, ω_2 are the humidity ratios (kg/kg).

After getting those correlations, the calculation of P_{AC} was depended on the room cooling load and the ambient temperature under Chiang Mai climate.

2.2 Energy Consumption of an Inverter Air conditioner Unit with Assisted PCM Packed Bed Cool Storage

The seasonal energy efficiency ratio (SEER) of the air conditioner with phase change material was also investigated for both charging and discharging periods.

2.2.1 Electrical power during charging period

The electrical power during charging period could determine following SEER equations above and based on the coolness absorption capacity of PCM packed bed in the solidification process, ambient temperature, and operating period in charging period. The PCM having a melting point around 18 °C was considered.

2.2.2 Electrical power during discharging period

After the charging period finished, the discharging period of PCM packed bed was immediately started, and the stored coolness was released by flowing the room air temperature through the packed bed then the heat removed by sensible heat of the evaporator coil was reduced. Therefore, the electrical power consumption and energy saving from PCM could be carried out. A set of thermostat temperature of 25 °C, SEER equations, and the ambient temperature were considered.

2.3 Mathematical Model of PCM Packed Bed Cool Storage

Figure 2.3 shows the unit with packed bed length (L) and cross-sectional area (A) contains spherical balls each having diameter (D_b) which generates a void fraction (ϵ). There is an air temperature at a given inlet air temperature and a mass flow rate entering the packed bed storage and exchanges heat with the PCM.

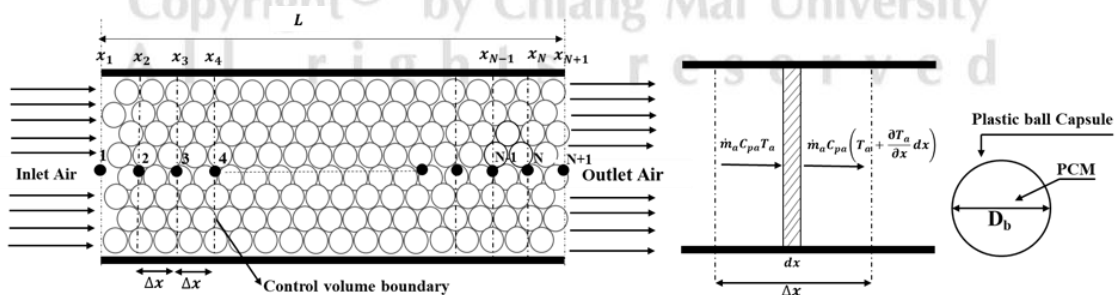


Figure 2.3 PCM packed bed storage.

When the bed is separated into N sections each having a cross-sectional area A , thickness of Δx and the bed temperature T_b is assumed to be uniform for the all section,

for air side, the energy balance at a control volume Adx when the bed is well insulated could be given in a form as

$$\dot{m}_a C_{pa} T_a = h_v (Adx) (T_a - T_b) + \dot{m}_a C_{pa} \left(T_a + \frac{\partial T_a}{\partial x} dx \right) \quad (2.7)$$

For convection heat transfer coefficient (h_v) in the ball bed. The experimental result of L6f and Hawley [15] was used as follows.

$$h_v = 650 \left(\frac{G}{D_b} \right)^{0.7} \quad (2.8)$$

Where G is mass flow rate per area of bed (kg/s.m^2), D_b is diameter of spherical ball (m).

From equation (2.7),

$$\frac{\partial T_a}{\partial x} = \left(-\frac{h_v A}{\dot{m}_a C_{pa}} \right) (T_a - T_b) \quad (2.9)$$

Boundary condition at $i = 1$: $x = x_1 \rightarrow T_a = T_{a,1}$

Boundary condition at $i = 2$: $x = x_2 \rightarrow T_a = T_{a,2}$

Boundary condition at $i = N - 1$: $x = x_{N-1} \rightarrow T_a = T_{a,N-1}$

Boundary condition at $i = N$: $x = x_N \rightarrow T_a = T_{a,N}$

$$\int_i^{i+1} \frac{\partial T_a}{(T_a - T_b)} = - \int_0^{\Delta x} \left(\frac{h_v A}{\dot{m}_a C_{pa}} \right) \partial x \quad (2.10)$$

$$\ln \frac{T_{a,i+1} - T_{b,i}}{T_{a,i} - T_{b,i}} = - \left(\frac{h_v A}{\dot{m}_a C_{pa}} \right) \Delta x \quad (2.11)$$

$$\frac{T_{a,i+1} - T_{b,i}}{T_{a,i} - T_{b,i}} = \exp \left(- \frac{h_v A}{\dot{m}_a C_{pa}} \Delta x \right) \quad (2.12)$$

$$T_{a,i+1} = T_{b,i} + (T_{a,i} - T_{b,i}) \exp \left(- \frac{h_v A}{\dot{m}_a C_{pa}} \Delta x \right) \quad (2.13)$$

Where i and $i+1$ are the entering and the exit of the i^{th} section, respectively of the bed having a thickness Δx (m). $T_{a,i}$ and $T_{a,i+1}$ are the inlet and outlet air temperatures at any section of the packed bed ($^{\circ}\text{C}$), respectively. \dot{m}_a is the air mass flow rate flowing through the packed bed (kg/s) and C_{pa} is the air specific heat capacity (kJ/kg K).

Consider the PCM packed bed, the energy balance of the PCM packed bed with heat transfer rate from air to PCM packed bed of thickness Δx could be formed in term of enthalpy ($h_{b,i}$) as

$$\dot{m}_a c_{p_a} (T_{a,i}^t - T_{a,i+1}^t) = M_b \frac{dh}{dt} \quad (2.14)$$

$$\dot{m}_a c_{p_a} (T_{a,i}^t - T_{a,i+1}^t) = \rho_b A \Delta x (1 - \varepsilon) \left(\frac{h_{b,i}^{t+\Delta t} - h_{b,i}^t}{\Delta t} \right) \quad (2.15)$$

$$h_{b,i}^{t+\Delta t} - h_{b,i}^t = \frac{\dot{m}_a c_{p_a} (T_{a,i}^t - T_{a,i+1}^t)}{\rho_b A \Delta x (1 - \varepsilon)} \Delta t \quad (2.16)$$

$$h_{b,i}^{t+\Delta t} = h_{b,i}^t + \frac{\dot{m}_a c_{p_a} (T_{a,i}^t - T_{a,i+1}^t)}{\rho_b A \Delta x (1 - \varepsilon)} \Delta t \quad (2.17)$$

Where $h_{b,i}^t$ and $h_{b,i}^{t+\Delta t}$ are the specific enthalpies of the PCM (kJ/kg) at time t (s) and time $t + \Delta t$ (s), respectively. ρ_b is the PCM density (kg/m³).

The temperature of PCM varied with the phase change as shown in Figure 2.4. Thus, the PCM packed bed temperature of each period could be calculated by enthalpy as follows.

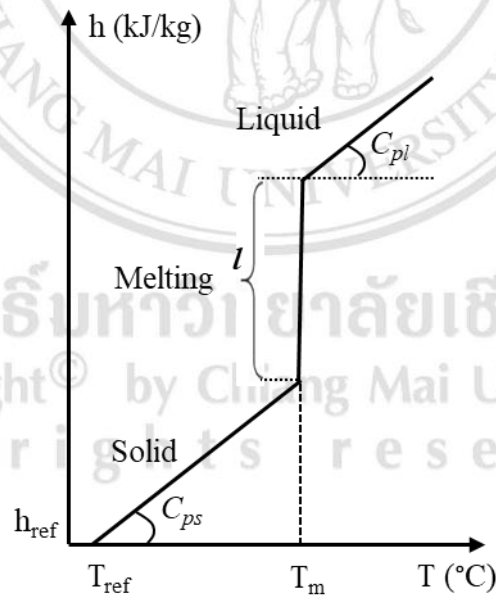


Figure 2.4 Enthalpy with a various temperature of PCM in each phase change.

- Solid phase

$$\begin{cases} h_{ref} \leq h_{b,i}^{t+\Delta t} < Cp_s(T_m - T_{ref}) \\ T_{ref} \leq T_{b,i}^{t+\Delta t} < T_m \end{cases} \quad (2.18)$$

The variant temperature of PCM at solid phase

$$h_{b,i}^{t+\Delta t} - h_{b,i}^t = Cp_s (T_{b,i}^{t+\Delta t} - T_{b,i}^t) \quad (2.19)$$

$$T_{b,i}^{t+\Delta t} = T_{b,i}^t + \frac{h_{b,i}^{t+\Delta t} - h_{b,i}^t}{Cp_s} \quad (2.20)$$

$$T_{b,i}^{t+\Delta t} = T_{b,i}^t + \frac{\dot{m}_a Cp_a (T_{a,i}^t - T_{a,i+1}^t)}{\rho_b A \Delta x (1 - \varepsilon) Cp_s} \Delta t \quad (2.21)$$

$T_{b,i}^t = T_{ref}$ and $h_{b,i}^t = h_{ref} = 0$ at the initial condition.

- Melting Zone

$$Cp_s (T_m - T_{ref}) \leq h_{b,i}^{t+\Delta t} \leq Cp_s (T_m - T_{ref}) + l \quad (2.22)$$

The temperature at melting point $T_{b,i}^{t+\Delta t} = T_m$

- Liquid phase

$$\begin{cases} h_{b,i}^{t+\Delta t} > Cp_s (T_m - T_{ref}) + l \\ T_{b,i}^{t+\Delta t} > T_m \end{cases} \quad (2.23)$$

The variant temperature of PCM at liquid phase

$$h_{b,i}^{t+\Delta t} - h_{b,i}^t = Cp_l (T_{b,i}^{t+\Delta t} - T_{b,i}^t) \quad (2.24)$$

$$T_{b,i}^{t+\Delta t} = T_{b,i}^t + \frac{h_{b,i}^{t+\Delta t} - h_{b,i}^t}{Cp_l} \quad (2.25)$$

$$T_{b,i}^{t+\Delta t} = T_{b,i}^t + \frac{\dot{m}_a Cp_a (T_{a,i}^t - T_{a,i+1}^t)}{\rho_b A \Delta x (1 - \varepsilon) Cp_l} \Delta t \quad (2.26)$$

Where T_{ref} is the PCM initial temperature ($^{\circ}\text{C}$), T_m is the melting temperatures during the phase change ($^{\circ}\text{C}$). Cp_s and Cp_l are the specific heat capacities of PCM in solid and liquid phases (kJ/kg K), respectively. l is the PCM latent heat (kJ/kg).

With the properties of the air entering the packed bed, the PCM properties, the initial packed bed temperature, the bed thickness and the temperature of air leaving the packed bed, $T_{a,i+1}^t$ then the PCM packed bed temperature after the time lapse Δt , $T_{b,i}^{t+\Delta t}$, could be evaluated from the above equations and the flow chart for the simulation is given in Figure 2.5 below.

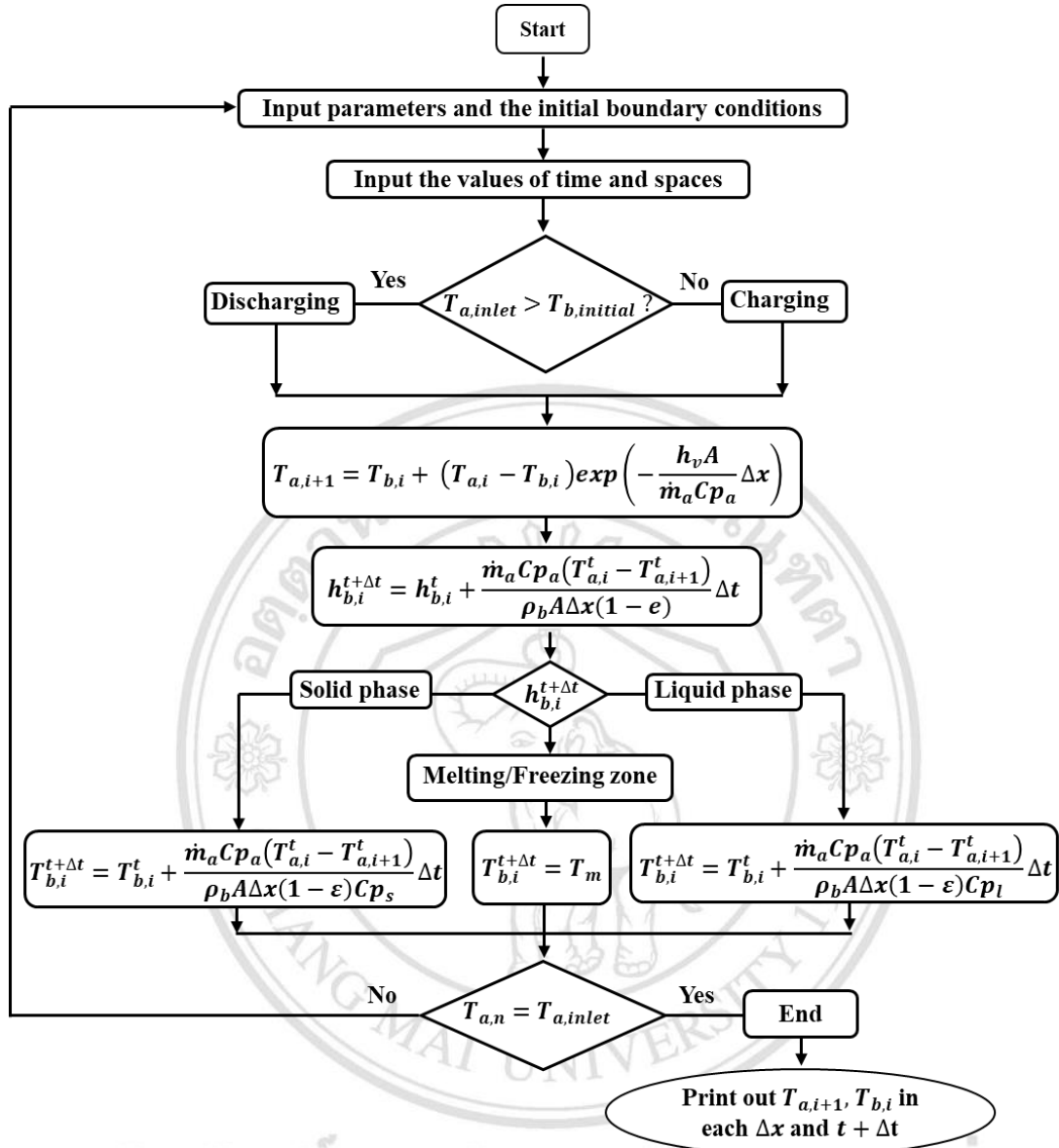


Figure 2.5 Flowchart of the simulation program for evaluating the PCM bed temperature and the air leaving PCM bed temperature during charging and discharging periods.

2.4 Electrical Power Equation of PV Module

The output power of solar PV could be provided by Osterwald's method [16] which could be formed as

$$P_{PV} = P_{max,STC} [1 - \gamma(T_C - 25)] \frac{I_T}{I_{STC}} \quad (2.27)$$

Where P_{PV} is the calculated output power (W), $P_{max,STC}$ is the maximal rated power at STC (Standard Test Conditions) which is given by manufacturer (W), I_T is a solar

radiation intensity on the module plane (W/m^2), I_{STC} is the references solar radiation intensity at 1000 (W/m^2), γ is a temperature coefficient of power ($^{\circ}\text{C}^{-1}$) and T_C is the solar module temperature ($^{\circ}\text{C}$).

For calculating the solar module temperature T_C the following linear model [17] was commonly used

$$T_C = T_{amb} + (NOCT - 20^{\circ}) \frac{I_T}{I_{NOCT}} \quad (2.28)$$

Where T_C is the solar module temperature($^{\circ}\text{C}$), T_{amb} is the ambient temperature($^{\circ}\text{C}$), $NOCT$ is the normal operating cell temperature given by the manufacturer ($^{\circ}\text{C}$), I_T is the solar radiation (W/m^2) and I_{NOCT} is the solar radiation intensity at 800 (W/m^2).

The instantaneous ambient temperature T_{amb} can be calculated and simulated from the maximum and the minimum temperatures on each day as

$$T_{amb}(t) = \frac{1}{2} \left[(T_{max} + T_{min}) + (T_{max} - T_{min}) \sin \left(\frac{2\pi}{24} (t - 9) \right) \right] \quad (2.29)$$

Where, T_{max} and T_{min} are the maximum and the minimum ambient temperatures ($^{\circ}\text{C}$) for Chiang Mai as given in Table 2.1.

Table 2.1 The maximum and the minimum ambient temperatures of Chiang Mai, Thailand [18].

Month	T_{max}	T_{min}
January	29.8	14.9
February	32.7	16.2
March	35.2	19.5
April	36.5	22.9
May	34.2	23.8
June	32.7	24
July	31.8	23.9
August	31.5	23.7
September	31.7	23.2
October	31.4	22.2
November	30.1	19.2
December	28.6	15.7

The solar energy incidence on a tilted surface could be divided into three components, beam radiation, diffuse radiation and reflected radiation from the ground. So, the solar radiation on a tilted surface (I_T) at any time could be calculated from the following equation as

$$I_T = I_b R_b + I_d \left(\frac{1 + \cos \beta}{2} \right) + I \rho_g \left(\frac{1 - \cos \beta}{2} \right) \quad (2.30)$$

Where I_b is the beam radiation on a horizontal surface (W/m^2), I_d is the diffuse radiation on a horizontal surface (W/m^2), β is the tilt angle, ρ_g is the ground reflectance and is taken to be 0.7 for all the months and R_b is the ratio of beam radiation on a tilted surface to that on a horizontal surface.

2.5 Economic Analysis

The present expenses of the system came from initial investment, yearly operation, and maintenance cost minus the salvage value of the system at the present worth.

$$C = C_{inv} + C_{o\&m} - C_{sv} \quad (2.31)$$

Where C is the present worth total cost (baht), C_{inv} is the present worth initial investment cost (baht), $C_{o\&m}$ is the present worth operation and maintenance cost (baht), and C_{sv} is the present worth salvage value (baht).

The annual expense of the system comes from the conversion of present value to the annual expense.

$$C_{annual} = C \times \frac{i(1+i)^n}{[(1+i)^n - 1]} \quad (2.32)$$

Where C_{annual} is the total annual expense (baht/year), i is the discount rate (%), and n is the service life of the system.

The unit cost of a product could be calculated as the following

$$C_{product} = \frac{\text{annual expenses}}{\text{annual product amount}} \quad (2.33)$$

2)

CHAPTER 3

Experimental Set-Up

This chapter, the experimental construction, measurement points and equipment testing were described in this section.

3.1 Experimental Construction

The experimental unit was constructed to conduct the tests as shown in Figure 3.1 compared to the conventional air conditioner unit in Figure 3.2. The room dimension was 3.9m x 3.4m x 2.9m. Four modules of solar PV were concurrently connected with the conventional electrical grid to power the air conditioner inside a testing room with a capacity of 1-ton TR without batteries storage. When the PV module cannot generate the electricity, then the electrical grid could provide the power directly to the load demand. The PV module unit will work efficiently following the condition of 18°47' south-facing level as the inclination angle for the panels (Tilt angle) under the latitude of Chiang Mai, Thailand. For the PCM energy cool storage was integrated with the air conditioner to reduce the air temperature before entering evaporator coil. The PCM packed bed cool storage contained spherical balls having a diameter of 40mm and melting point was around 18°C. The utilization of the PCM cool storage was divided into 2 periods. The first period was known as charging period which acted during the off-peak cooling load in the early morning as closed loop cycle. The cool air from the evaporator coil employed to cool the PCM packed bed. After the charging period was finished, the discharging period was continuously started by flowing the room air temperature through the PCM packed bed storage in a purpose of reducing the air temperature before entering the evaporator coil, then the electrical consumption of the air conditioner was rather low. Consequently, the electrical power from PV modules and the PCM energy cool storage played a significant role in energy saving.

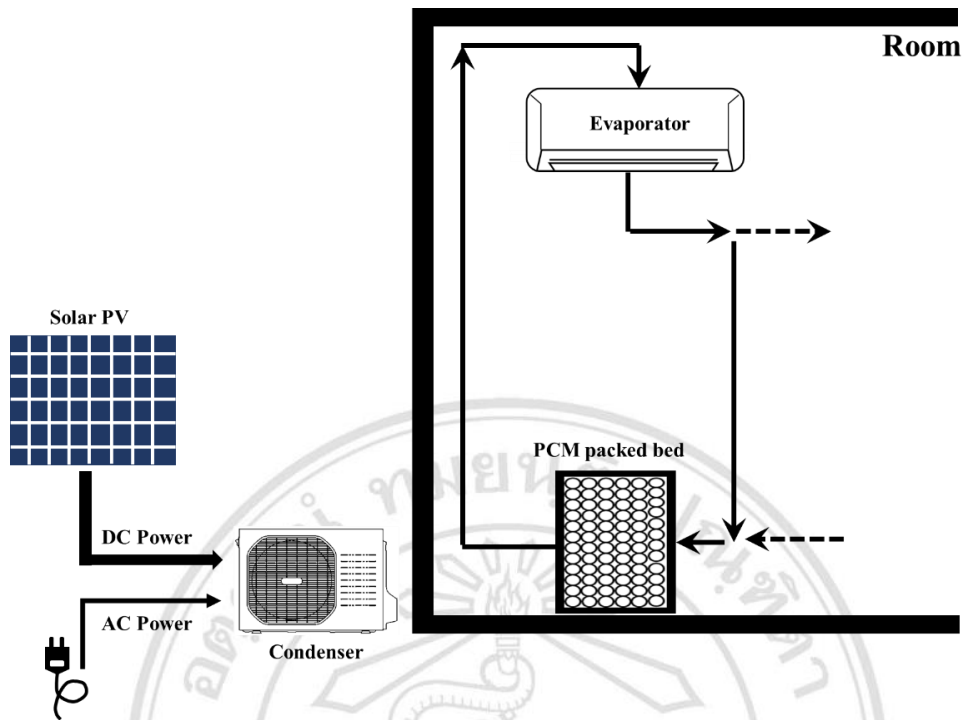


Figure 3.1 Schematic sketch of the modified air conditioner unit in the present study.

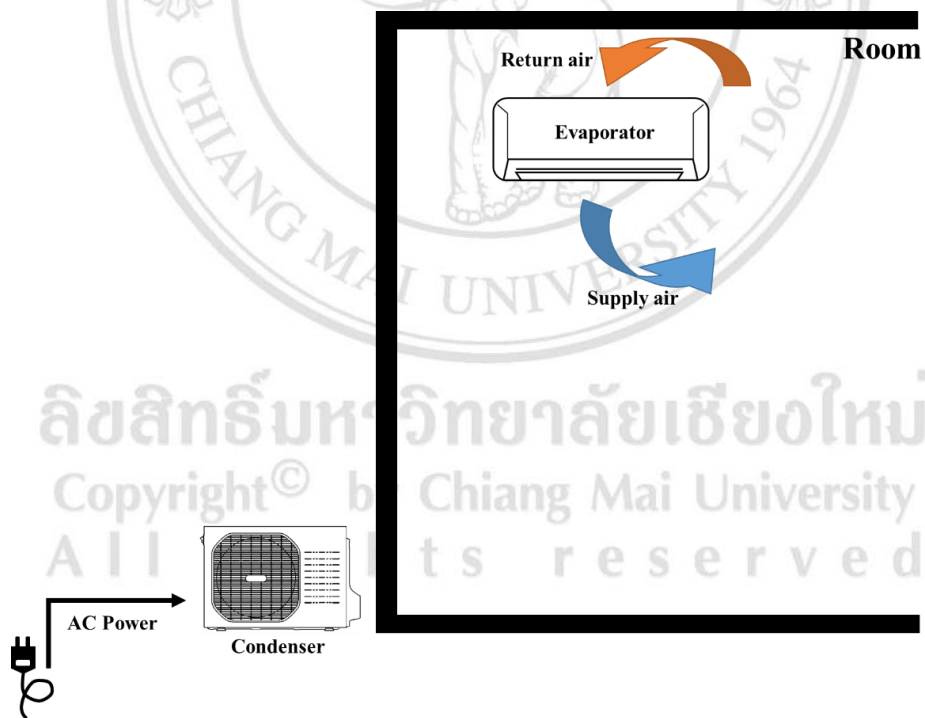


Figure 3.2 Schematic sketch of the conventional air conditioner unit.

3.2 Conventional Inverter Air Conditioner Unit

For coefficients, $a_1, a_2, a_3, b_1, b_2,$ and b_3 of SEER equation could be determined from experimental work under the Chiang Mai climate. The electrical power supplied to the

air conditioner (P_{AC}), room air temperature (T_r), dry bulb temperature (T_{db}), wet bulb temperature (T_{wb}), ambient temperature (T_{amb}), and air mass flow rate (\dot{m}_a) were measured as shown in Figure 3.3.

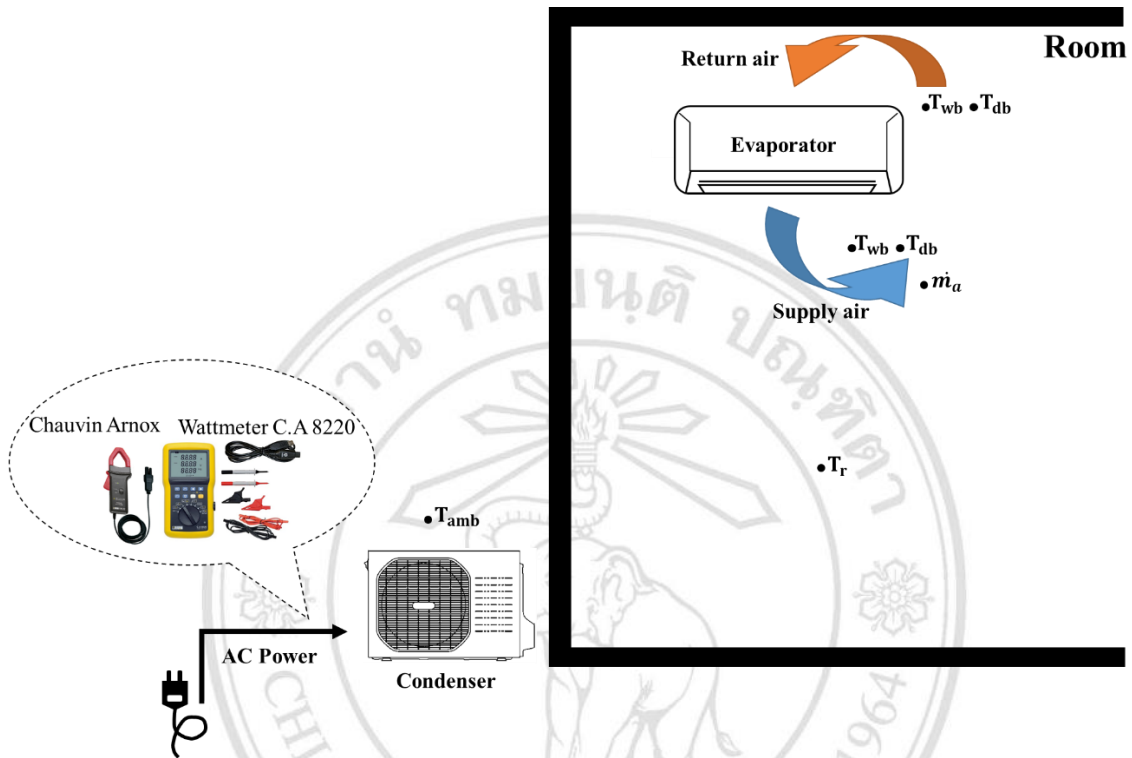


Figure 3.3 Measurement points of a conventional air conditioner.

The electrical heater having capacity around 1.5kW and the humidity controller were mainly used in this testing unit as indicates in Figure 3.4 and Figure 3.5. The heating load was coming from electrical heater and used for heating the room temperature. The humidity in the room was set to be 60 % following the comfort zone requirement.



Figure 3.4 Humidity controller.



Figure 3.5 Electrical heater.

3.3 PCM Packed Bed Cool Storage

The dimension of the PCM packed bed was 0.6 m x 0.5 m x 0.24 m. The PCM packed bed was located under the evaporator coil as shown in Figure 3.6. The phenomena of PCM packed bed in charging and discharging periods were determined. The thickness of 0.08 m, 0.16 m, 0.24 m and air mass flow rate were considered in the tested work.

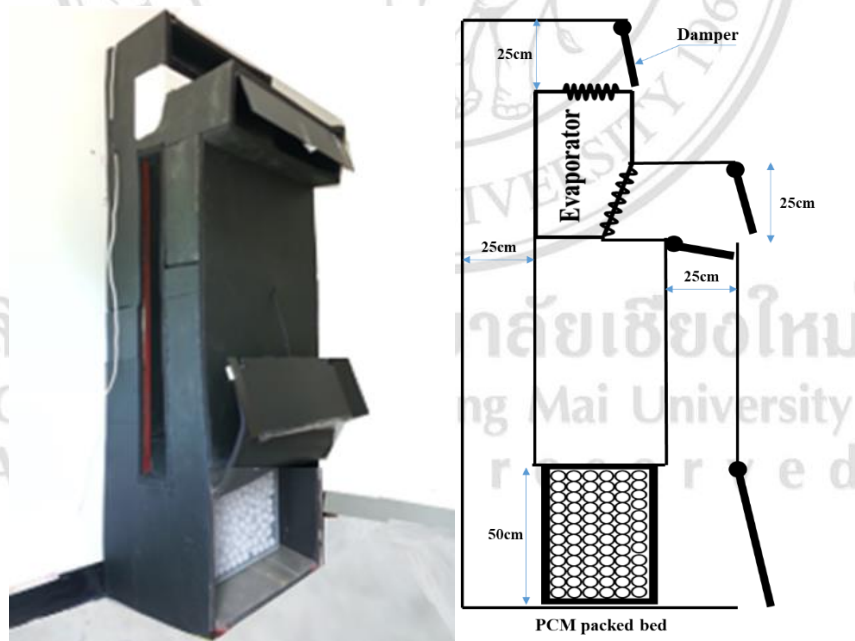


Figure 3.6 Integration of the PCM packed bed and the evaporator coil.

3.3.1 Charging period

The leaving air temperature around 5°C from the evaporator coil circulated through the packed bed as a closed loop cycle to solidify the PCM packed bed during off-peak

period at the early morning during the charging period, all PCM balls in packed bed was initially in a liquid state then the charging cycle was started until it reached to the inlet air temperature. The charging period and the measurement points of the unit indicate in Figure 3.7.

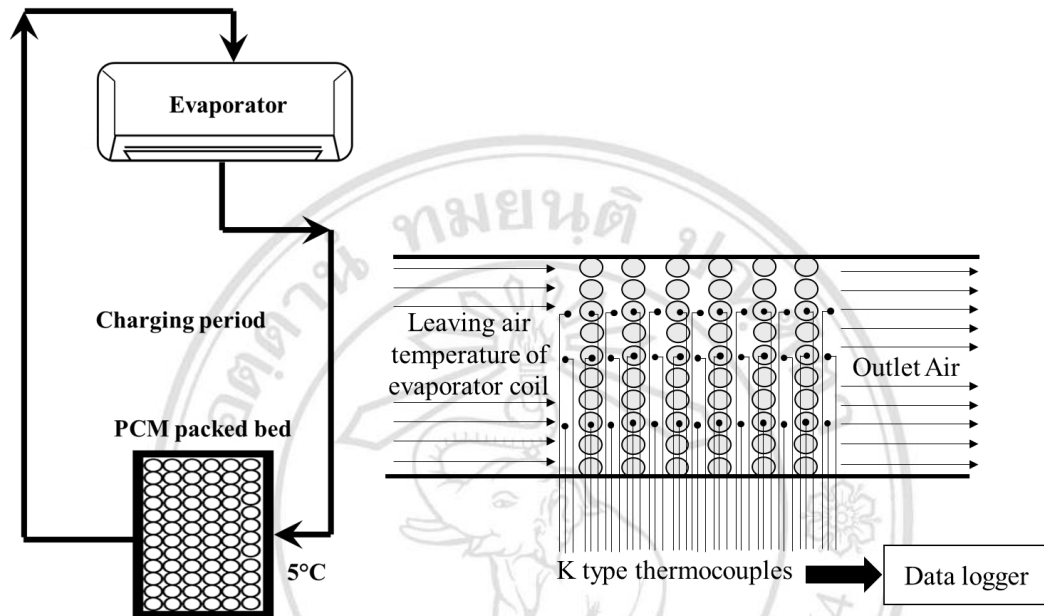


Figure 3.7 Charging period of the PCM packed bed and measurement temperature points of the air and PCM packed bed.

3.3.2 Discharging period

The room air temperature at around 25 °C in a testing room was flowed through the packed bed then the PCM packed bed begun to melt and released the cool air to the evaporator as discharging period. This period was ended up when the leaving air temperature of the packed bed reached to the room air temperature. The discharging period of the PCM packed bed and the measurement points of the unit illustrate in Figure 3.8

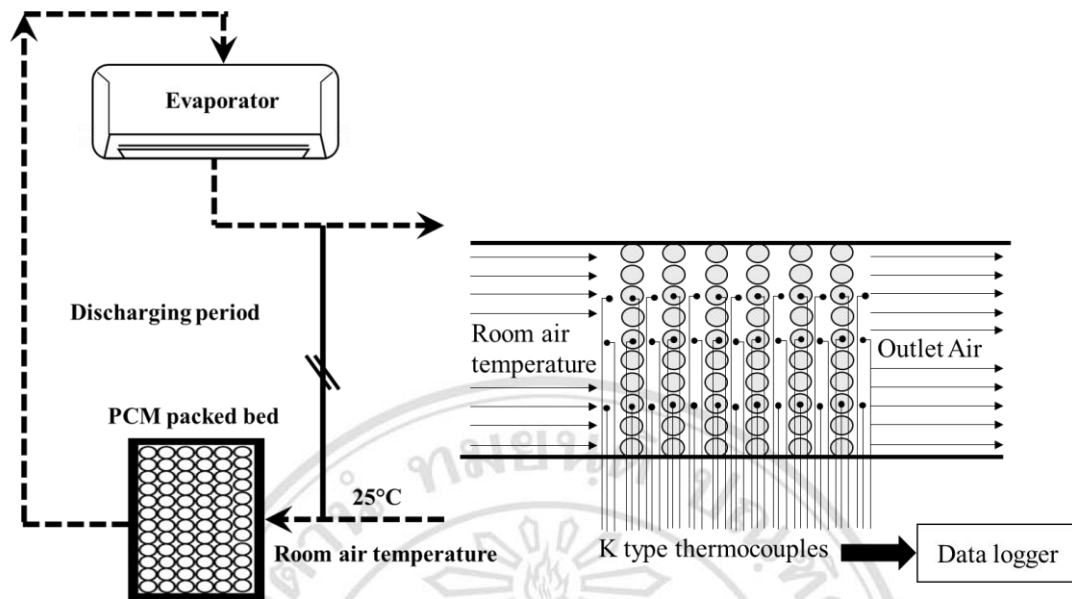


Figure 3.8 Discharging period of the PCM packed bed and measurement temperature points of the air and PCM packed bed.

From those of the experimental testing and its phenomena, the appropriate thickness could be determined. The total time of discharging period could be carried out when the outlet air temperature of the PCM packed bed was around 25 °C.

3.4 Solar PV Connected Grid Line

This unit was all direct current (DC) designed. The total direct current (DC) power from solar PV modules can be generated directly into the air conditioning unit without any converter for an alternating current (AC) power input. This can be reduced the energy loss in power convertor by more than 30% [19]. The unit was automatically switched to electrical grid when solar energy was not enough to operate in air conditioning unit. Four modules of the solar PV and 1-ton of refrigeration (TR) were considered in this experimental work. The electrical power output of PV modules for air conditioner under Chiang Mai condition could be carried out. The description of the unit and its components are given in Figure 3.9.

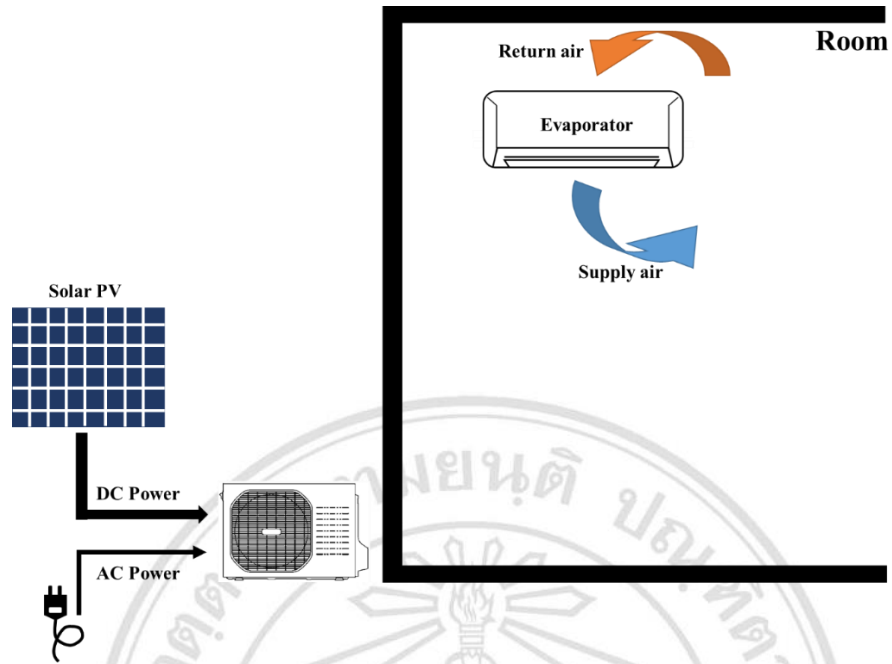


Figure 3.9 On-grid solar PV powered the air conditioner.

The output power of PV module (P_{PV}), the solar radiation incidence on the module (I_T), the module temperature (T_C) and the ambient temperature (T_{amb}) were measured under the latitude at Chiang Mai as given in Figure 3.10.

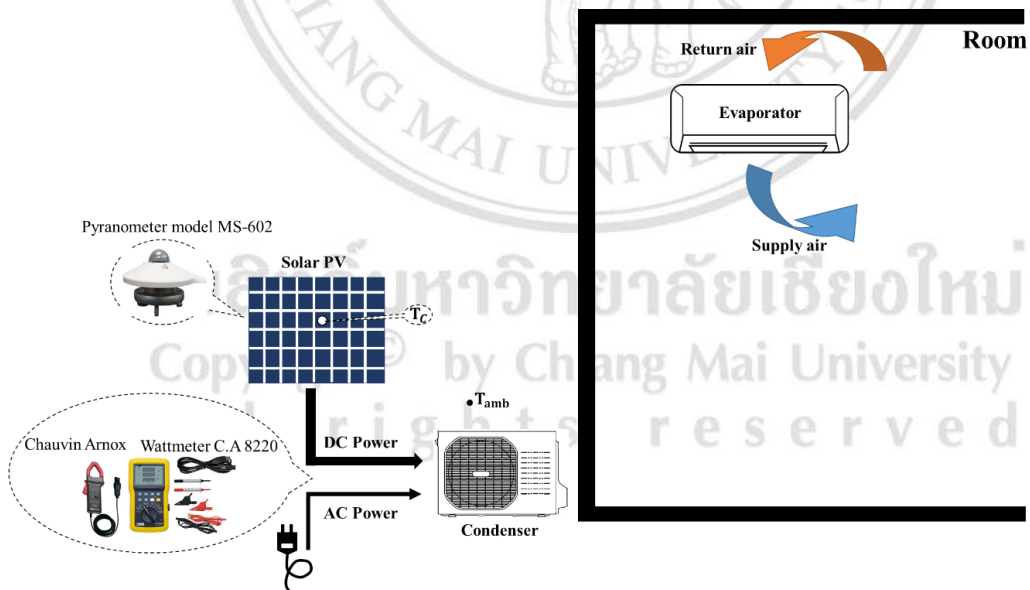


Figure 3.10 Schematic diagram of measurement points.

3.5 Experimental Components

The main components of the unit were PV modules, 1-TR of the inverter air-conditioner, and phase change material PCM RT-18 HC.

3.5.1 Air conditioner

The most common type of the air conditioner is technically referred to the vapor-compression refrigeration system as shown in Figure 3.11. The experiment conducted with the inverter air conditioner and the operating speed of compressor depended upon the ambient temperature. As the compressor ran on varies speed thus the power utilization was rather low compared to the fixed speed compressor of the air conditioner.

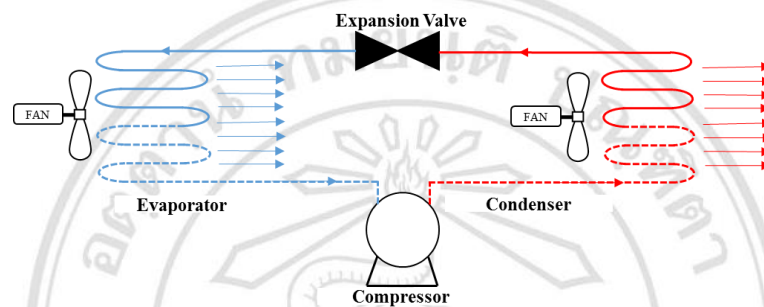


Figure 3.11 Basic of air conditioning cycle.

R-410A air conditioner having a capacity around 1-TR (12,000 BTU/h) with air-cooled condenser was used in this experiment. The unit was separated into two sections for the evaporator (indoor unit) and condenser (outdoor unit). The description of air conditioner is given in Table 3.1.

Table 3.1 Descriptions of the inverter air conditioner R-410a.

Components	Details
Model	PKSM12
Rated Voltage	220V-240V
Rated Frequency	50Hz
Cooling Capacity	3500W
Heating Capacity	3800W
Cooling Power Input	880W
Heating Power Input	950W
Cooling Rated Input	1260W
Heating Rated Input	1600W
Weight	43kg

3.5.2 PV module

Solar (or photovoltaic) cells convert the sun's energy into electricity. A solar cell is a sandwich of n-type silicon and p-type silicon. It generates electricity by using sunlight to make electrons hop across the junction between the different flavors of silicon as shown in Figure 3.12. When sunlight shines on the cell, photons (light particles) bombard the upper surface. The photons carry the energy down through the cell in which the giving up the energy to electrons in the lower, p-type layer. The electrons use this energy to jump across the barrier into the upper, n-type layer and escape out into the circuit.

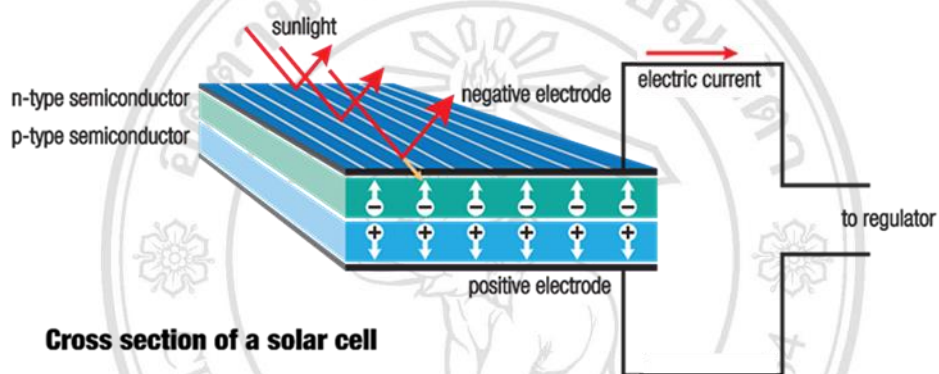


Figure 3.12 Schematic diagram of solar cell [20].

The PV modules polycrystalline were used in this experimental work as shown in Figure 3.13 with the detail of the specification in Table 3.2.



Figure 3.13 Series of a PV modules for the unit.

Table 3.2 Specification of PV module.

TSM-320PD14		
Maximum Power	(P_{max})	320W
Maximum Power Voltage	(V_{mp})	37.1V
Maximum Power Current	(I_{mp})	8.63A
Open Circuit Voltage	(V_{oc})	45.8V
Short Circuit Current		9.10A
Maximum Series Fuse		15A
Power Selection		0-5W
Module Application		Class A
Maximum System Voltage		IEC 1000V
NOCT (Normal Operating Cell Temperature)		44°C ($\pm 2^\circ\text{C}$)
Temperature Coefficient of P_{max}		- 0.41%/°C
Electrical Rating at SCT AM=1.5 IRRADIANCE=1000W/m ² Temp=25 °C		

3.5.3 PCM RT-18 HC

The PCM was considered as thermal energy storage (TES). It stored and released thermal energy during melting and solidification processes. Phase change materials released large amounts of energy during its phase change in form of latent heat. This enabled for heat or cold energy storages that was stored from one process or period and kept for the later use.

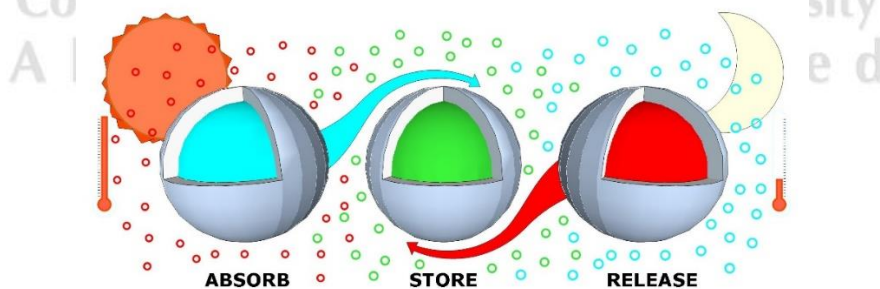


Figure 3.14 Store and release of phase change material cycle [3].

PCM RT-18HC having the melting point around 18 °C was selected to be the cool storage. The concept of using its latent to reduce the air before entering the evaporator coil could be carried out. The PCM balls in this experiment were made of plastic ball diameter of 40 mm. The properties of PCM RT-18HC detail in Table 3.3

Table 3.3 Descriptions of the RT-18HC.

RT18HC	Properties
Melting point	18 °C
Heat storage capacity $\pm 7,5\%$	260 kJ/kg
Specific heat capacity	2 kJ/ (kg K)
Density solid at 15 °C	0.88 kg/l
Density liquid at 25 °C	0.77 kg/l
Heat conductivity (both phases)	0.2 W/ (m K)
Volume expansion	12.5 %
Max. operation temperature	50°C

3.6 Measuring Instrument

The measurement of the experimental data in the unit performance was measured by some instruments tool such as pyranometer model MS-602, k type thermocouples, wattmeter C.A 8220, Chauvin Arnox PAC 93, data-logger model Huato S220-T8 and hotwire anemometer am-4234sd as shown in Figure 3.15 and Table 3.4.

ลิขสิทธิ์มหาวิทยาลัยเชียงใหม่
Copyright© by Chiang Mai University
All rights reserved



Figure 3.15 Measuring instruments.

Table 3.4 Measurement range and accuracy of instruments.

Instrument tools	Range	Accuracy
Pyranometer	(0 ~ 2000) W/m ²	(± 0.05)
K type thermocouple	(-200~1300) °C	(±1.5)
Data-logger S220-T8	(-200~+1800) °C	(±1°C±5%)
Wattmeter C.A 8220	(6 ~ 600) Vrms	± (0.5 % +2 counts)
Chauvin Arnox PAC 93	(1 ~1200) A	
Hot wire anemometer	(0.2~35) m/s	±(5%+a), a=0.1 m/s

3.6.1 Research procedure

This experiment was going to find the energy consumption of the air conditioning unit and study the phenomena behaviours of the PCM packed bed in purpose of finding the appropriate thickness and the operating time in charging and discharging periods. The PV power output for air conditioning unit was also carried out. Thus, the electrical saving could be determined. The research procedure is given in Figure 3.16.

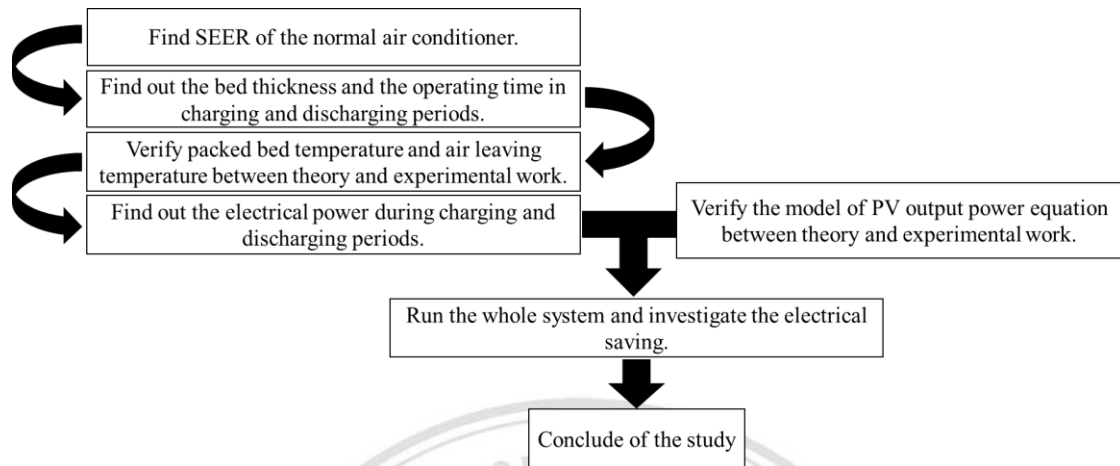


Figure 3.16 Flowchart of the study process.

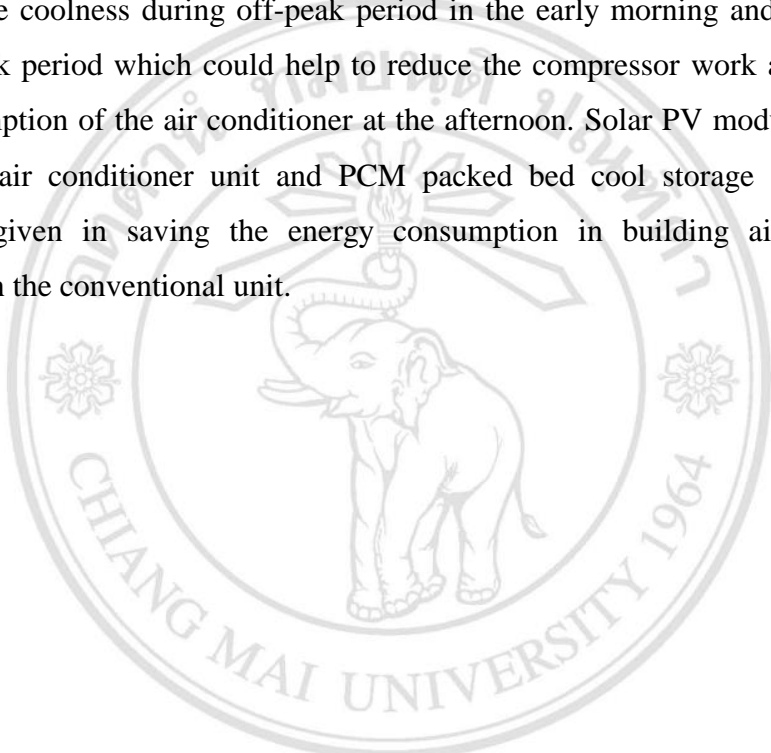
The experiment begins to operate under these conditions:

- Four PV modules was supplied the electrical power to air conditioner and PCM packed bed was also integrated with the air conditioning unit in the testing room.
- The electrical heater having capacity around 1.5 kW and the humidity was controlled to be 60% were considered in the testing room.
- The experimental work was started up from 5:00 am-4:00 pm.
- The experiment was operated in condition of clear sky day, partly cloudy day and mostly cloudy day.
- The experimental data acquisition unit such as pyranometer, K type thermocouples, data-logger, power meter and hot wire anemometer, and pyranometer were used.
- The temperature data-loggers were used to record the dry bulb temperature, wet bulb temperature, room temperature, PCM packed bed temperature, outlet air temperature of PCM packed bed, ambient temperature and module temperature in every 1 minute.
- The pyranometer, power meter, and hot wire anemometer were used to measure the solar radiation, electrical power, and air velocity, respectively in every 1 minute.
- Experiment testing
- Comparison of the simulated results from the developed model with those of the experiment.

- Sizing of the PV modules and the appropriate thickness of the PCM packed bed for the air conditioner from the developed model.
- Conclude of the study.

3.6.2 Expected results

On-grid solar power unit could reduce large amount of the energy consumption in the building air conditioner with faster payback period. The PCM packed bed cool storage could store the coolness during off-peak period in the early morning and release back during on-peak period which could help to reduce the compressor work as well as the power consumption of the air conditioner at the afternoon. Solar PV module connected grid line for air conditioner unit and PCM packed bed cool storage assisted were significantly given in saving the energy consumption in building air conditioner compared with the conventional unit.



ลิขสิทธิ์มหาวิทยาลัยเชียงใหม่
Copyright© by Chiang Mai University
All rights reserved

CHAPTER 4

Thermal Characteristics on Charging and Discharging of RT-18 HC

PCM Packed Bed Cool Storage

This chapter, thermal characteristics of air charging/discharging period could be considered by enthalpy method. The correlations of dimensionless terms for the PCM packed bed were used to predict the outlet air temperature of the bed and the total operating period of both charging/discharging periods.

4.1 Charging Period

In the experiment, the packed bed storage was fully charged in the off-peak period. At the beginning of the charging period, the temperature of the PCM inside the spherical ball was equaled to the ambient temperature, which was in the liquid phase. The inlet air temperature of 5°C into the packed bed was considered. As the low inlet air temperature was passing through the packed bed, the molten PCM begun to solidify and released heat. The packed bed temperatures dropped down quickly at the beginning as sensible heat form until they approached the PCM freezing point. The latent heat form displayed at the freezing point temperature of the packed bed storage which remaining a constant temperature at around 18 °C. After that the temperatures decreased quickly again and closed to the inlet air temperature at around 5 °C. The simulated results also agreed to experimental data with the mean absolute percentage error (MAPE) less than 10%. as indicates in Figure 4.1.

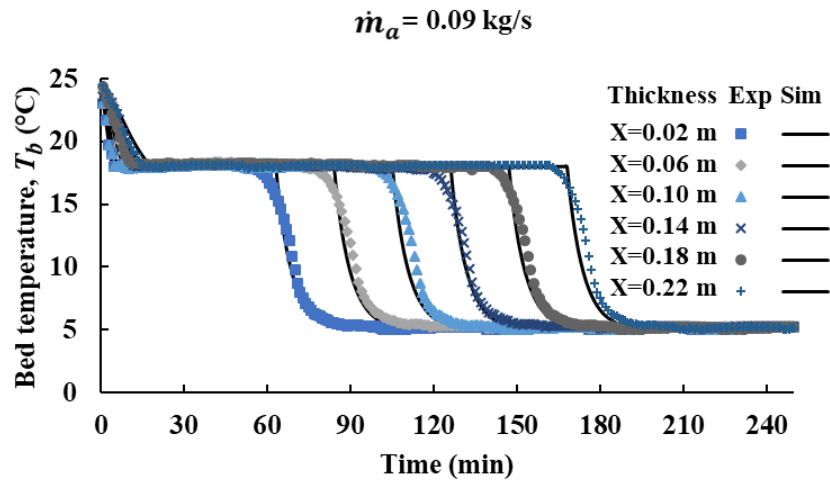


Figure 4.1 Variation of bed temperature with time at various bed thicknesses during charging period.

Figure 4.2 also shows the outlet air temperature leaving the packed bed when the inlet air temperature was 5 °C. Due to the heat transfer of temperature difference between the inlet air and the packed bed was high, the outlet air temperature decreased faster at the initial period. After the bed temperature reached the phase change, the outlet air temperature dropped slowly at any section of the packed bed.

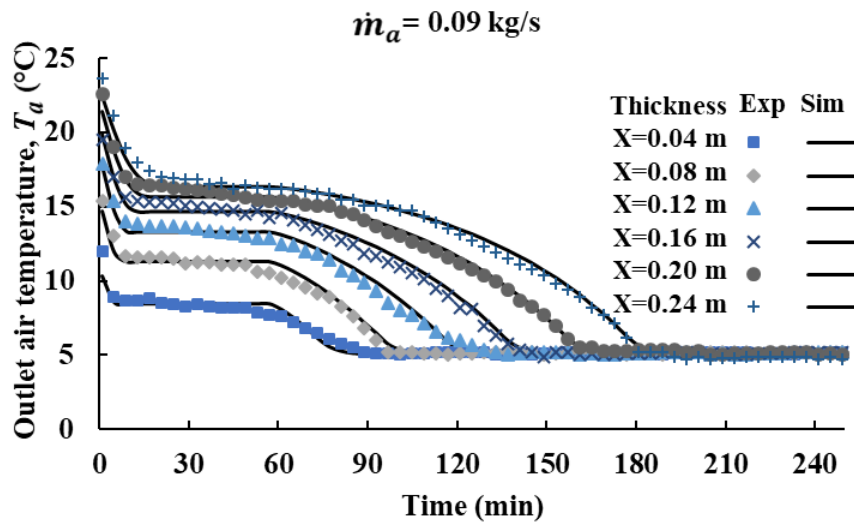


Figure 4.2 Variation of outlet air temperature with time at various thicknesses during charging period.

Figure 4.3 presents the solidification time of the paraffin from the initial temperature at 25 °C to the end of freezing point at 18 °C with the inlet air temperature at 5 °C. It could be noted that the total solidification time was reduced approximately around

32.22-36.96% at thicknesses of 0.02-0.24 m, respectively, when the mass flow rate increased from 0.056-0.093 kg/s.

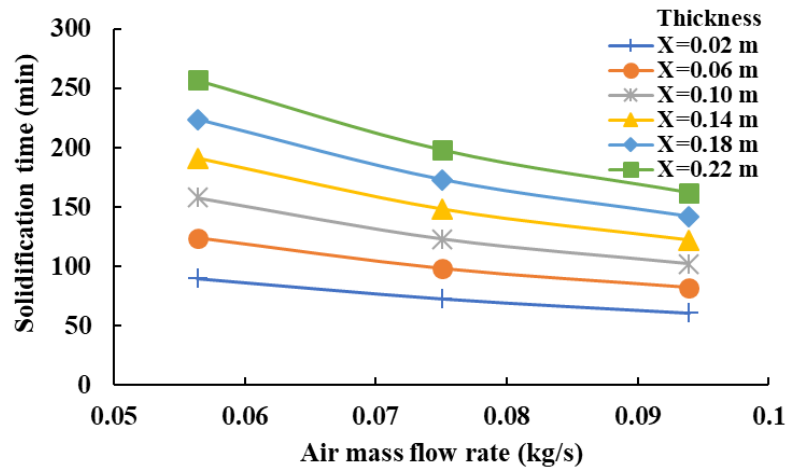


Figure 4.3 Effect of mass flow rates on PCM charging period.

The above data was consolidated into dimensionless terms of θ , τ and Y as illustrated in Figure 4.4. θ is the dimensionless which comes from the temperature ratio of the inlet temperature minus the outlet air temperature and the inlet air temperature minus the melting temperature. τ is the dimensionless of heat transfer between air and PCM bed with the PCM latent heat. Y is the dimensionless term illustrating the heat transfer coefficient with mass flow rate and its specific heat capacity during the charging period. From the Figure, a correlation could be determined as

$$\begin{aligned} \theta(\tau, Y) = & 0.03 - 0.17\tau + 0.92Y + 0.89\tau^2 - 0.93\tau Y - 0.16Y^2 - 0.99\tau^3 + 0.88\tau^2 Y \\ & + 0.11\tau Y^2 + 0.31\tau^4 - 0.2\tau^3 Y - 0.13\tau^2 Y^2 - 0.03\tau^5 + 0.01\tau^4 Y \\ & + 0.03\tau^3 Y^2 \end{aligned} \quad (4.1)$$

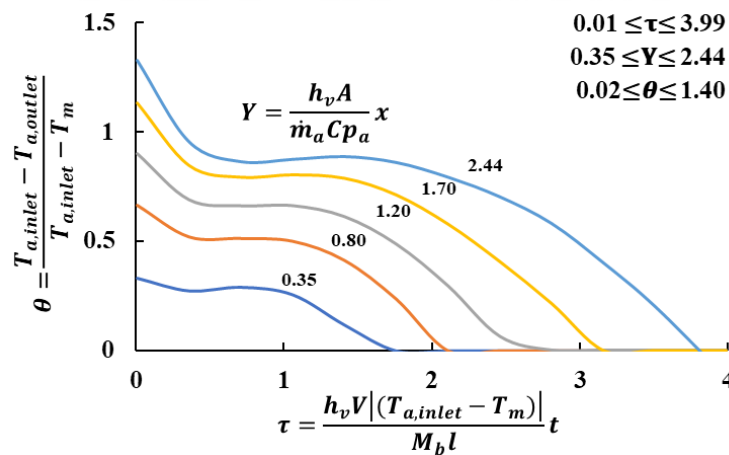


Figure 4.4 Dimensionless terms, θ , τ and Y (charging period).

From the correlation, with given values of the air mass flow rate and its inlet temperature, the bed dimension, the PCM properties, and the operating period, τ and Y could be calculated including θ then the outlet air temperature leaving the packed bed could be evaluated.

4.2 Discharging Period

Figure 4.5 shows the PCM temperature at the ball center of the PCM bed at various bed thicknesses during discharging period with the inlet temperature of 25 °C. The PCM temperature was initially raised up in the form of sensible heat and when it reached the temperature around 18 °C the phase change temperature was obtained. after that the temperature increased continually and approached the inlet air temperature. The temperature at higher thickness increased slowly compared to that of the previous section. It could be noted that the simulated results agreed quite well with the experiment data. The mean absolute percentage error (MAPE) was less than 10%.

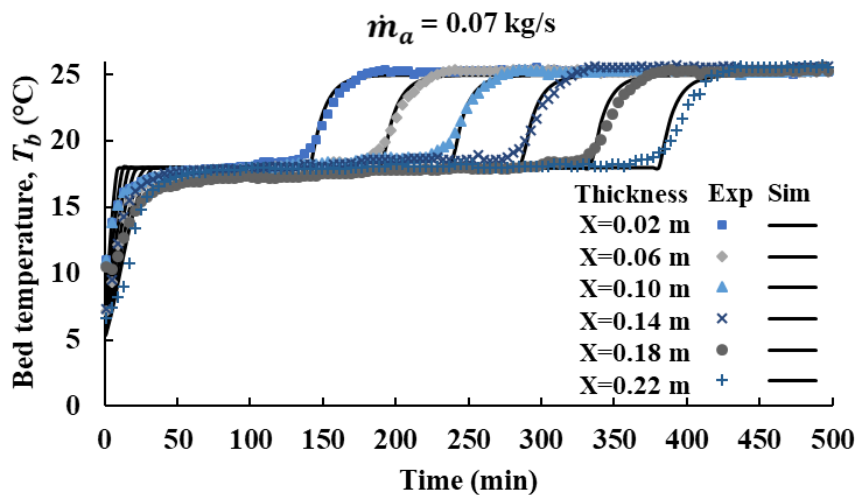


Figure 4.5 Variation of bed temperature with time at various bed thicknesses during discharging period.

Figure 4.6 shows the temperature profiles of the outlet air temperature flowing throughout the bed at any bed section. The simulation results showed a good agreement with the experimental data. The outlet air temperature at each thickness rose up quickly during the sensible heat period and slightly increased during the PCM phase change. Smaller the PCM thickness, shorter the time that the outlet air temperature was in equilibrium with the inlet air.

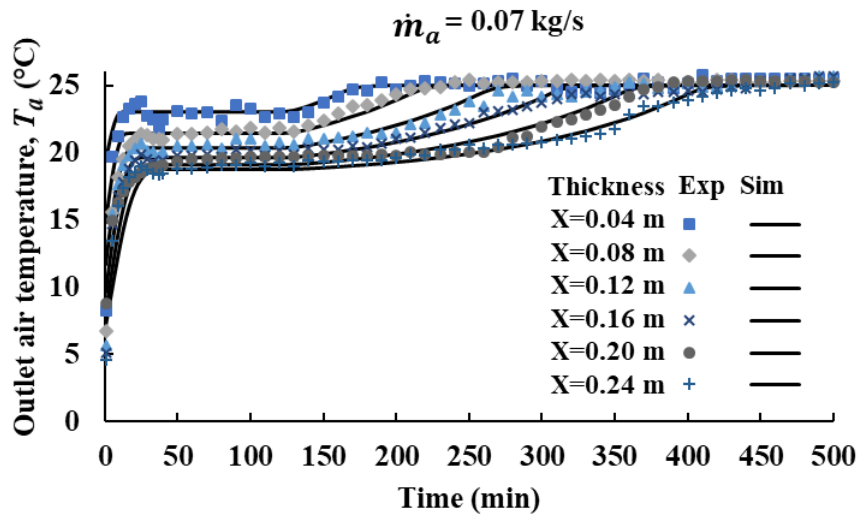


Figure 4.6 Variation of outlet air temperature with time at various thicknesses during discharging period.

Figure 4.7 shows the effects of air mass flow rate on the PCM melting time during PCM discharging period (from the initial temperature of 5 °C to the end of melting point at temperature of 18 °C). The total melting time was reduced approximately around 31.81-37.02% at thicknesses of 0.02-0.24m, respectively, when the mass flow rate increased from 0.052-0.087 kg/s. It could be seen that increase of the mass flow rate resulted in higher heat transfer rate then the solidification time could be shortened for all PCM thicknesses.

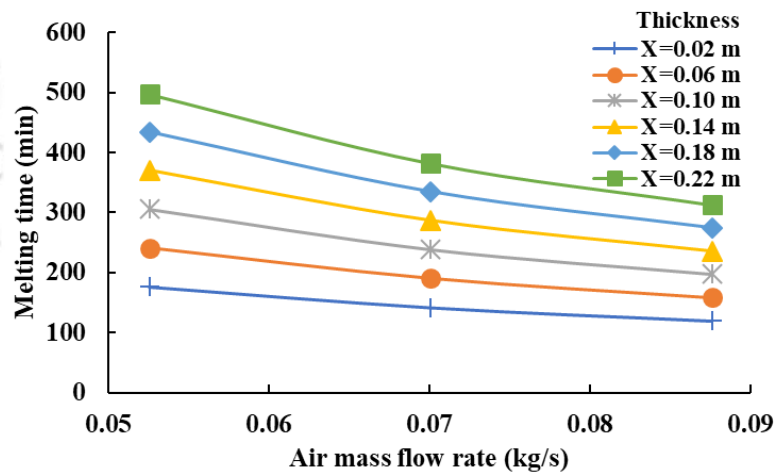


Figure 4.7 Effect of mass flow rates on PCM discharging period.

The correlation of the dimensionless terms, θ , τ and Y during the discharging period also presents in Figure 4.8 which could be formed as

$$\theta(\tau, Y) = 0.08 - 0.74\tau + 1.21Y + 2.44\tau^2 - 2.11\tau Y - 0.14Y^2 - 2.54\tau^3 + 2.38\tau^2 Y + 0.03\tau Y^2 + 0.96\tau^4 - 0.94\tau^3 Y - 0.04\tau^2 Y^2 - 0.13\tau^5 + 0.14\tau^4 Y + 0.003\tau^3 Y^2 \quad (4.2)$$

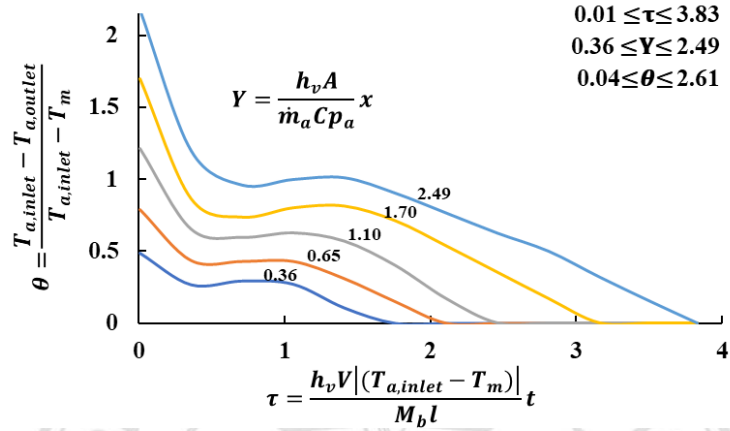


Figure 4.8 Dimensionless terms, θ , τ and Y (discharging period).

Similarly, with values of the air mass flow rate and the inlet temperature, the bed thickness, the operating period and the PCM properties, the values of τ , Y , θ and finally the outlet air temperature leaving the packed bed could be determined.

Figure 4.9 illustrates the inlet air temperature of evaporator coil at the thickness of 0.08 m, 0.16 m, and 0.24 m. From the experimental tests, more PCM bed thickness resulted in longer discharging period. The operating times during discharging period was 411 minutes when the thickness was 0.24 m. This showed that the inlet air temperature of evaporator coil could be maintained below 25 °C around 7 hours which was covered the whole day of the air conditioner operation. Therefore, the appropriate thickness could be considered at 0.24 m.

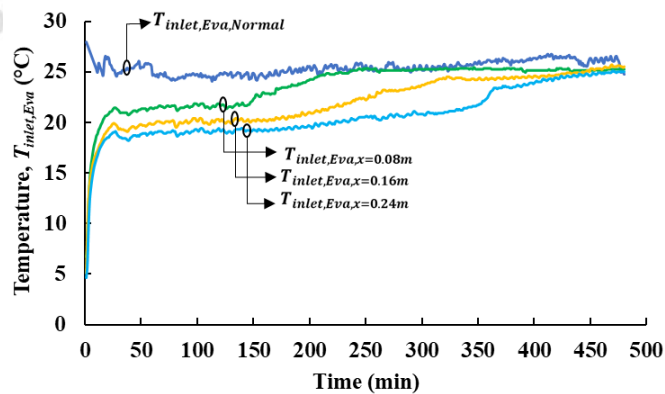


Figure 4.9 Experimental results of the inlet air temperature at the evaporator coil with and without PCM bed.

CHAPTER 5

Performance of Air Conditioner Unit with and without PCM Packed

Bed Cool Storage

This chapter, an R-410A air conditioner of 1 TR (12,000 BTU/h) with air-cooled condenser was experimentally studied its thermal performances under Chiang Mai weather. The energy saving of the air conditioner unit with assisted PCM packed bed cool storage was also evaluated.

5.1 Thermal Performance of the Conventional Air Conditioner Unit

In this experimental test a 1 TR inverter air conditioner having R-410a as a refrigerant was used. For inverter air conditioner the seasonal energy efficiency ratio SEER was considered in [27]. From the experimental results, it could be found that its SEER (ratio of the cooling capacity to the power input of the unit) could be set up as a function of surrounding ambient temperature as shown in Figure 5.1. It could be observed that as the ambient temperature increased, the SEER dropped down. These correlations were achieved at various ambient temperatures rank. Due to there was the inverter air conditioner ran at variable speeds then the correlation of the SEER could be formed as follows

Minimum speed of inverter compressor

$$SEER = -0.0955 T_{amb} + 6.6 \quad (5.1)$$

Inverter range

$$SEER = -0.0759 T_{amb} + 5.8 \quad (5.2)$$

Maximum speed of inverter compressor

$$SEER = -0.0492 T_{amb} + 4.7 \quad (5.3)$$

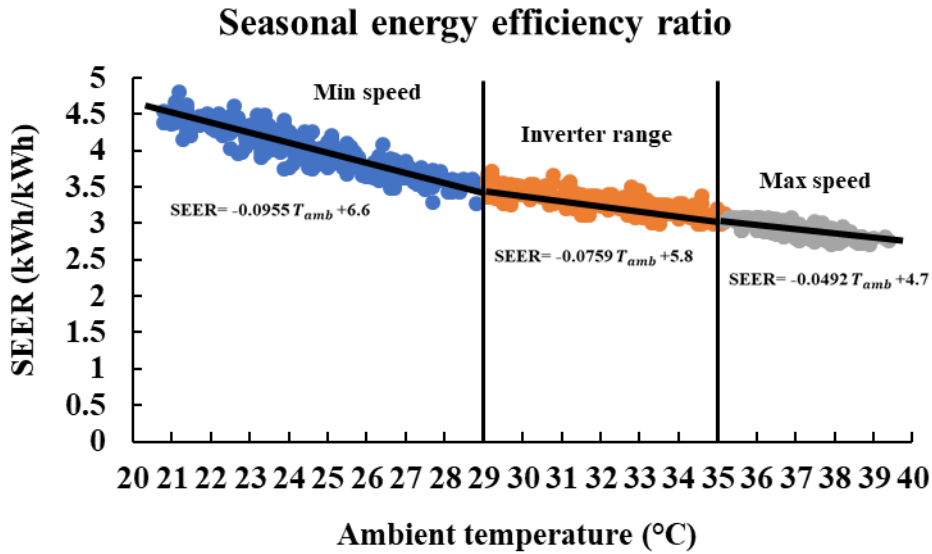


Figure 5.1 Thermal performance of the conventional inverter air conditioner unit.

Figure 5.2 and Figure 5.3 illustrate the electrical power consumption in summer and winter, respectively. In summer, the air conditioner generated with maximum power input around 1.2 kW due to the high ambient temperature. It could be noted that the calculated results match very well to the experimental data with mean absolute percentage error (MAPE) less than 10%.

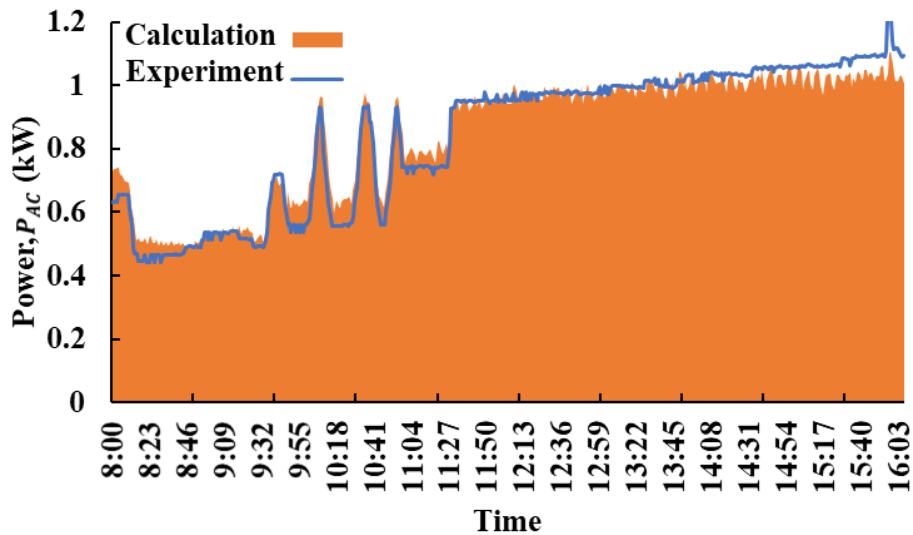


Figure 5.2 Electrical power of conventional inverter air conditioner unit in summer.

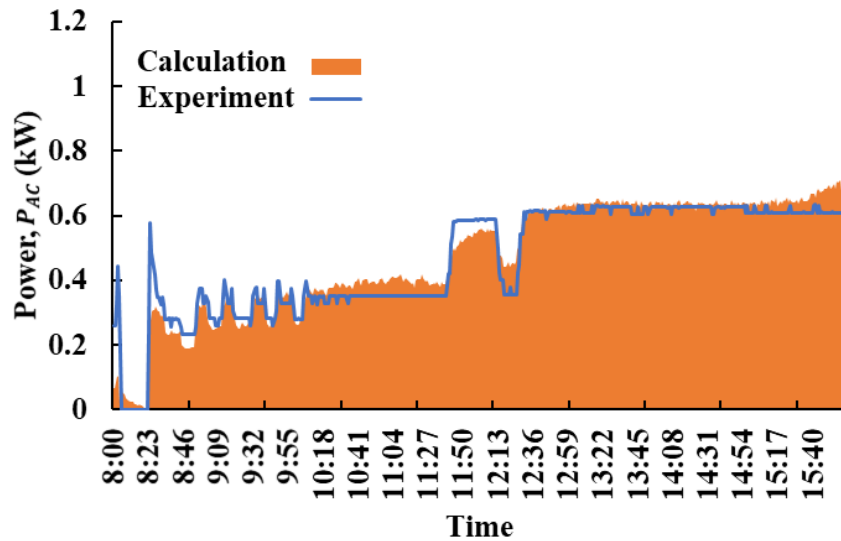


Figure 5.3 Electrical power of conventional inverter air conditioner unit in winter.

5.2 The Effect of PCM Bed Cool Storage on the Inverter Air Conditioner Operation

Following the PCM bed model and its dimensionless terms, the PCM bed cool storage was integrated with a 1 TR inverter air conditioner unit to reduce the cooling load at the evaporator and the electrical power from grid line. During the tested work, the internal load of the electrical heater around 1.5 kW, the controlled room temperature of 25 °C, 60% of humidity were considered. The tests were conducted for four consecutive days those had similar surrounding ambient temperature as given in Figure 5.4.

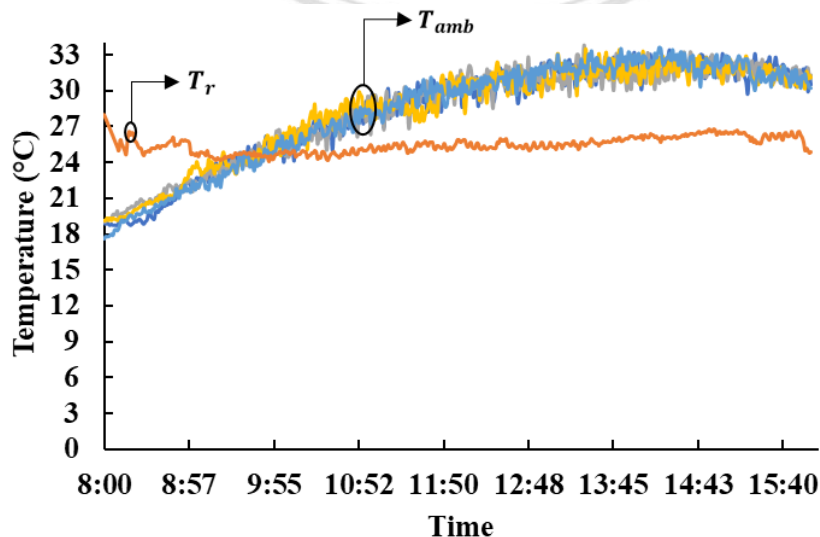
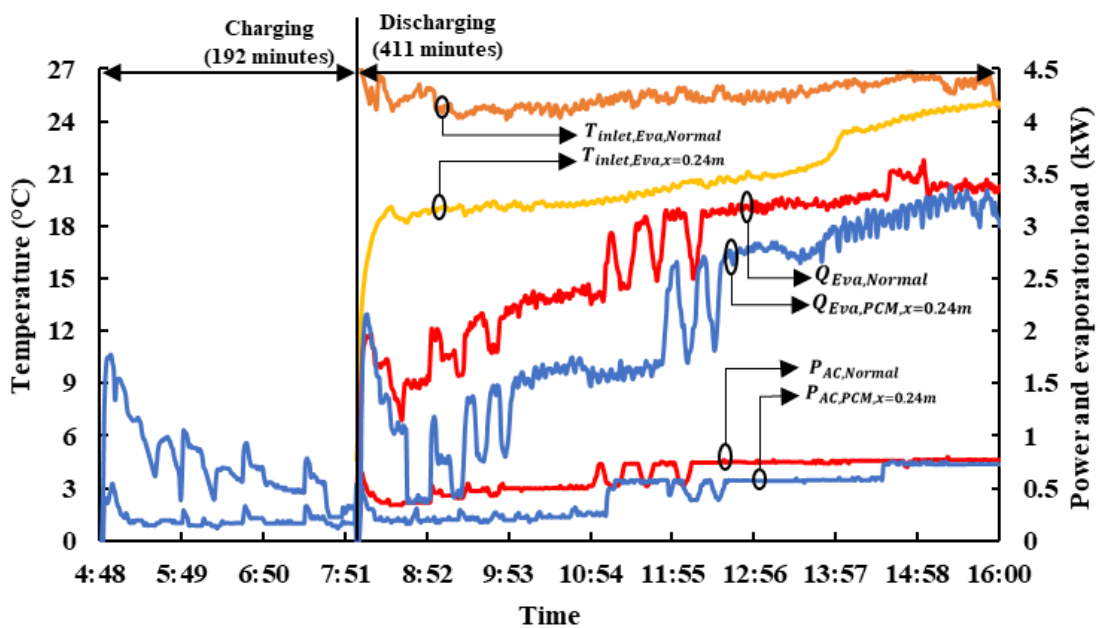


Figure 5.4 The room temperature and the surrounding ambient temperature during the tested work.

Figures 5.5 (a, b) show the cooling load performance and power consumption of the conventional air conditioner unit and the unit with assisted PCM bed at the thickness of 0.08 m and 0.24 m in winter. During the charging period, the PCM packed bed thickness of 0.08 m and 0.24 m needed around 96 minutes and 192 minutes, respectively, to complete the solidification. The inlet air temperature at the evaporator could be reduced the temperature below 25 °C around 210 minutes and 411 minutes when the thickness was 0.08 m and 0.24 m, respectively in discharging period. It could be noted that the inlet air temperature of the unit with assisted PCM bed was lower than the conventional unit. When the inlet air temperature of evaporator coil could be reduced, not only the cooling load but the electrical power consumption also reduced. The electrical power could be saved about 1.58-13.84% as thicknesses of 0.08-0.24 m. This confirmed that the PCM bed cool storage was potentially used from air conditioning unit.



(b)

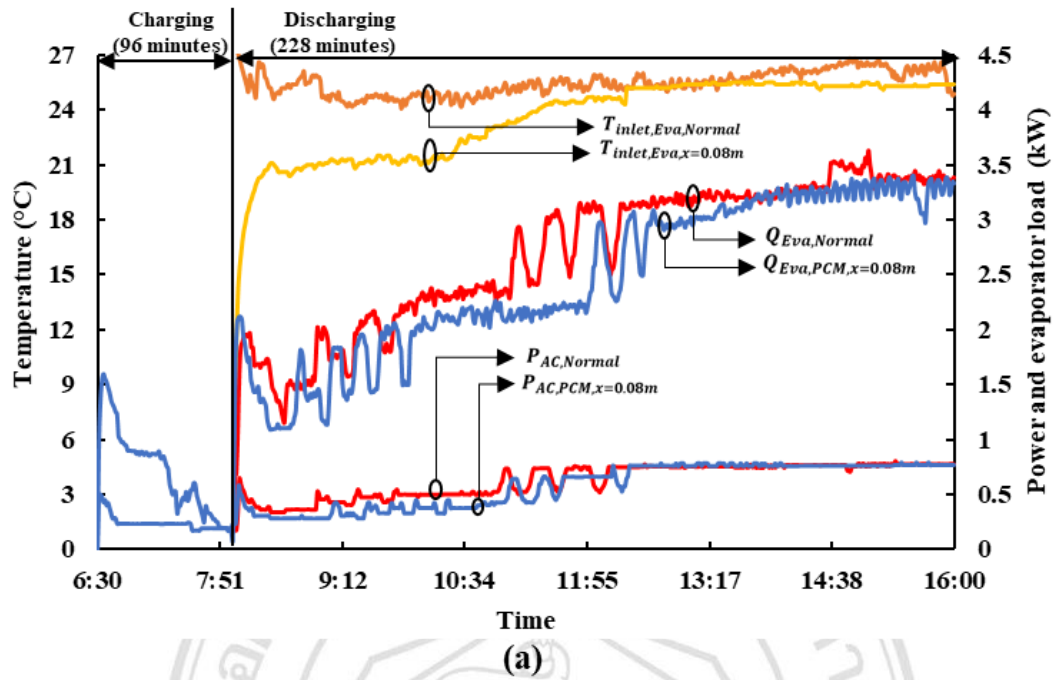


Figure 5.5 Experimental results of the conventional air conditioner unit with and without assisted PCM bed. (a) 0.08 m. (b) 0.24 m.

Table 5.1 shows the electrical power consumption of the normal unit and the unit with assisted PCM bed. The daily power consumption of the normal unit was around 5.04 kWh and those with assisted PCM bed thicknesses of 0.08 m, 0.16 m, and 0.24 m were 4.96 kWh, 4.18 kWh, and 4.34 kWh, respectively. It could be noted that the daily electrical power consumption could be saved around 1.58% to 13.84% when the assisted PCM bed thickness was 0.08 m to 0.24 m.

Table 5.1 Energy consumption of the air conditioner unit with and without assisted PCM bed cool storage.

Conventional unit		Thickness (m)	Charging period		Discharging period		Unit with assisted PCM bed		Saving (%)
Operating time	Total power (kWh)		Time (min)	Power (kWh)	Time (min)	Power (kWh)	Operating time	Total power (kWh)	
8:00am-4:00pm	5.04	X=0.08	96	0.36	228	4.60	6:30am-4:00pm	4.96	1.58
		X=0.16	149	0.52	324	4.18	5:30am-4:00pm	4.70	6.8
		X=0.24	192	0.63	411	3.71	5:00am-4:00pm	4.34	13.84

The sensible heat of the evaporator coil was reduced when the utilization of PCM bed was considered. In calculation of the total cooling load at the evaporator coil with assisted PCM bed, the inlet dry bulb temperature at the evaporator coil for the conventional air conditioner unit was replaced by the outlet air temperature of bed. With those of SEER correlations, then the electrical power during discharging period could be carried out in each month. For summer, the electrical power saving from grid line of the air conditioner with assisted PCM bed thickness of 0.08 m, 0.16 m, and 0.24 m were 4.91, 10.76, and 16.13%, respectively.

CHAPTER 6

PV Module Generation for Inverter Air conditioner Unit

This chapter, the validation of PV power output and module temperature were determined. The electrical power production of PV modules to air conditioner unit under the real weather condition in Chiang Mai was also carried out.

6.1 Validation of PV Power Generation and Module Temperature

Figure 6.1 gives solar radiation on tilt plan $18^{\circ}47'$ of PV modules and the ambient temperature on clear sky day. The solar radiation was obtained at around 8:00 am and the maximum point of solar radiation occurred around noon with the highest value by about 900-1000 W/m^2 .

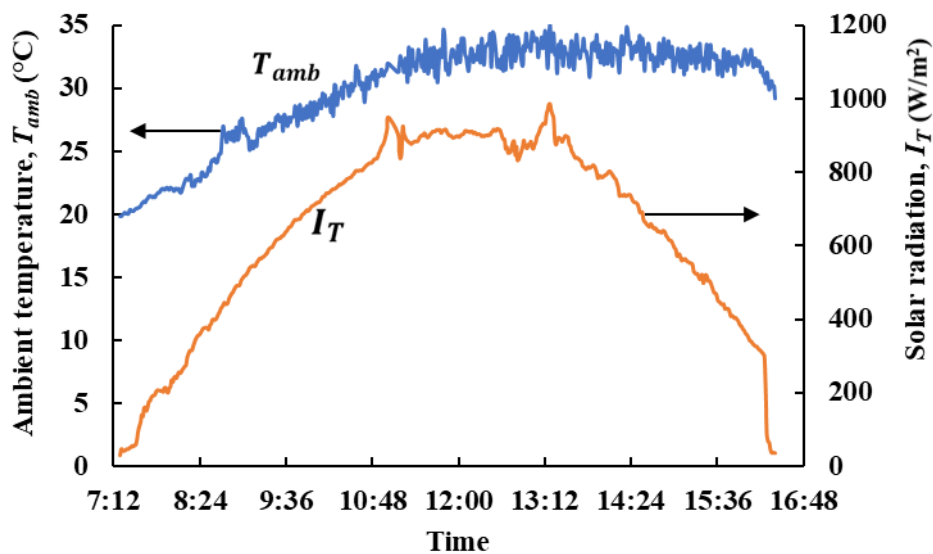


Figure 6.1 Ambient temperature and solar radiation on clear sky day.

The validation of the PV power output and module temperature from experimental data and formula showed a good agreement and a little bit error as given in the Figure 6.2. The results presented that the formula above can be used to predict the PV power output and the PV module temperature.

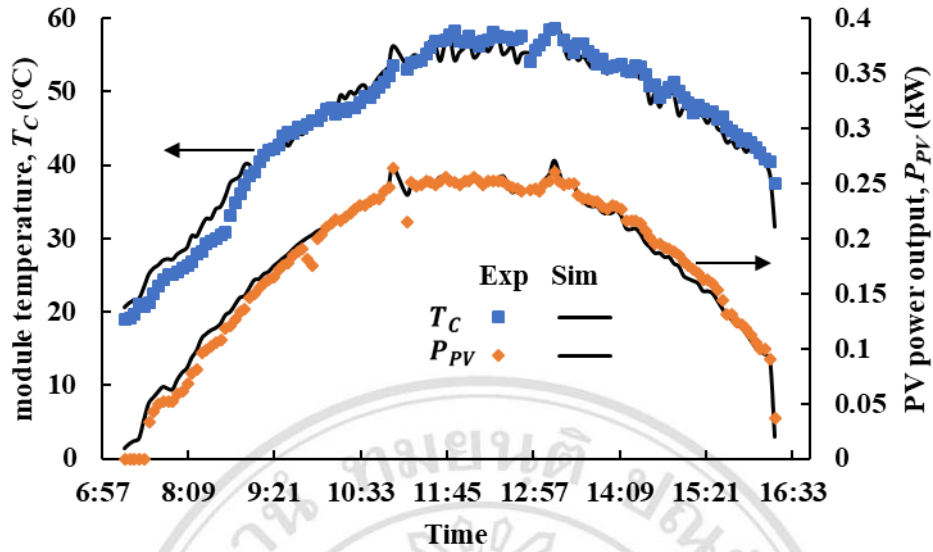
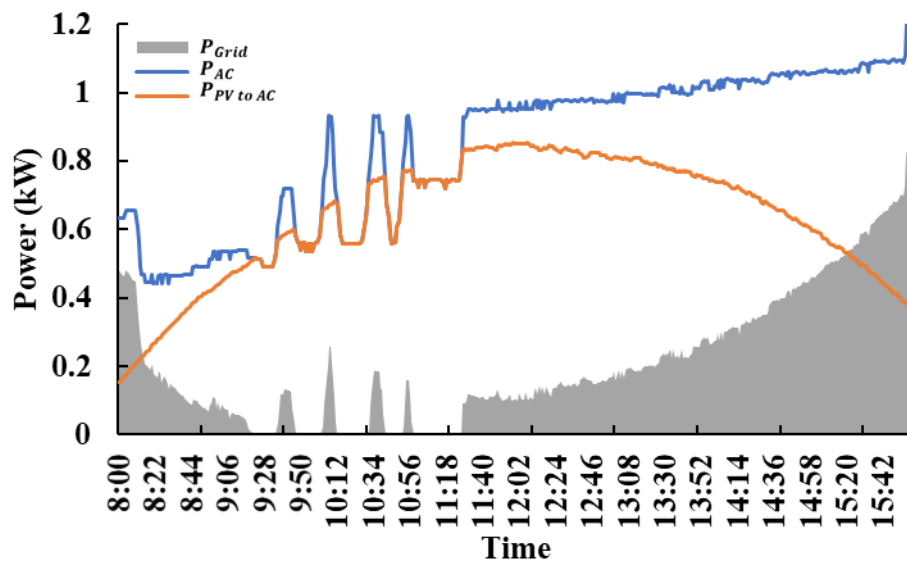


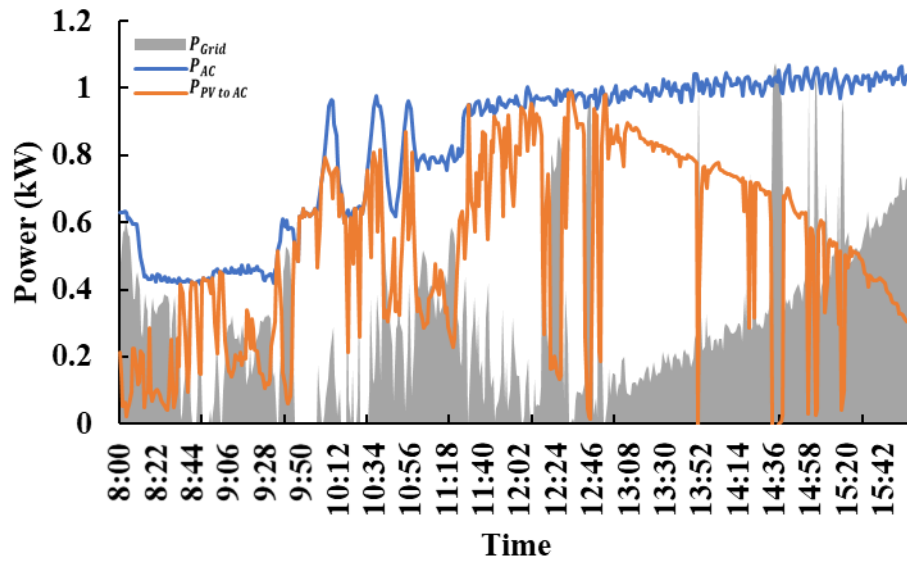
Figure 6.2 Validation of module temperature and PV power output.

6.2 Electrical Power Generation of PV Module

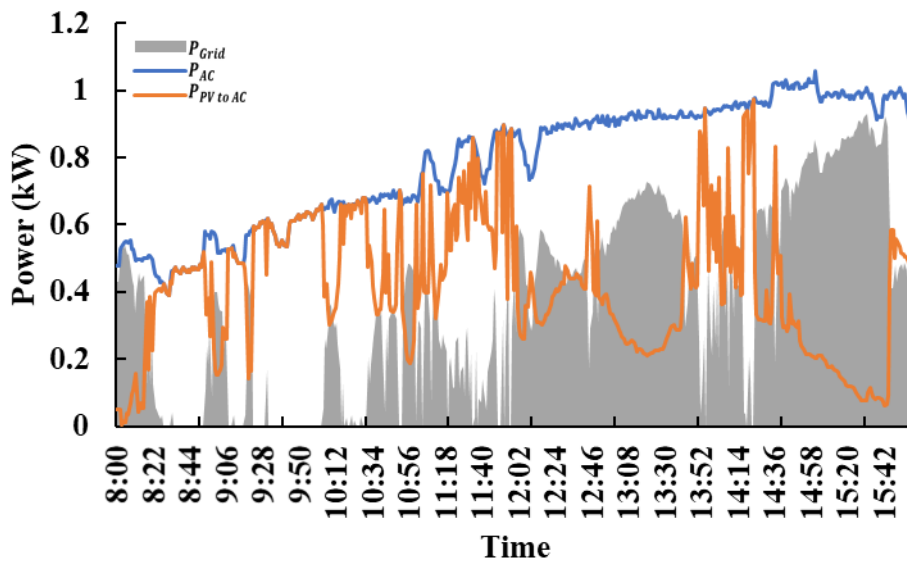
In condition of clear sky day, cloudy day, and mostly cloudy day, the electrical power of four PV modules could reduce the electrical from grid line during the summer about 75.13, 62.94, and 52.98%, respectively, as shown in Figure 6.3. It could be investigated that the PV modules could produce large amount of electrical power in clear sky day which was compared to the condition of cloud cover (mostly cloudy day). From the results, it could be noted that PV modules power production could match with the air conditioner load.



(a)



(b)



(c)

Figure 6.3 Electrical power reduction from grid line by four PV modules to air conditioner unit. (a) clear sky day. (b) cloudy day. (c) mostly cloudy day.

From Figure above, generally, the power generation of PV module was insufficient in the early morning and the late afternoon. A peak PV module power generation was from 11:00 am to 1:00 pm in the afternoon, maximum power-consuming of the air conditioning could be pointed at the late afternoon (1:00 pm -3:00 pm) since the high ambient temperature was obtained.

Figure 6.4 illustrates the electrical power requirement of air conditioner unit, PV power output, and the electrical power needed from grid line. The electrical power requirement of the air conditioner in summer was higher than the winter while the PV modules could produce large amount of electrical power in winter due to high solar radiation performance. The results showed that the electrical power from grid line could be reduced around 98.83% and 72.86% in winter and summer, respectively.

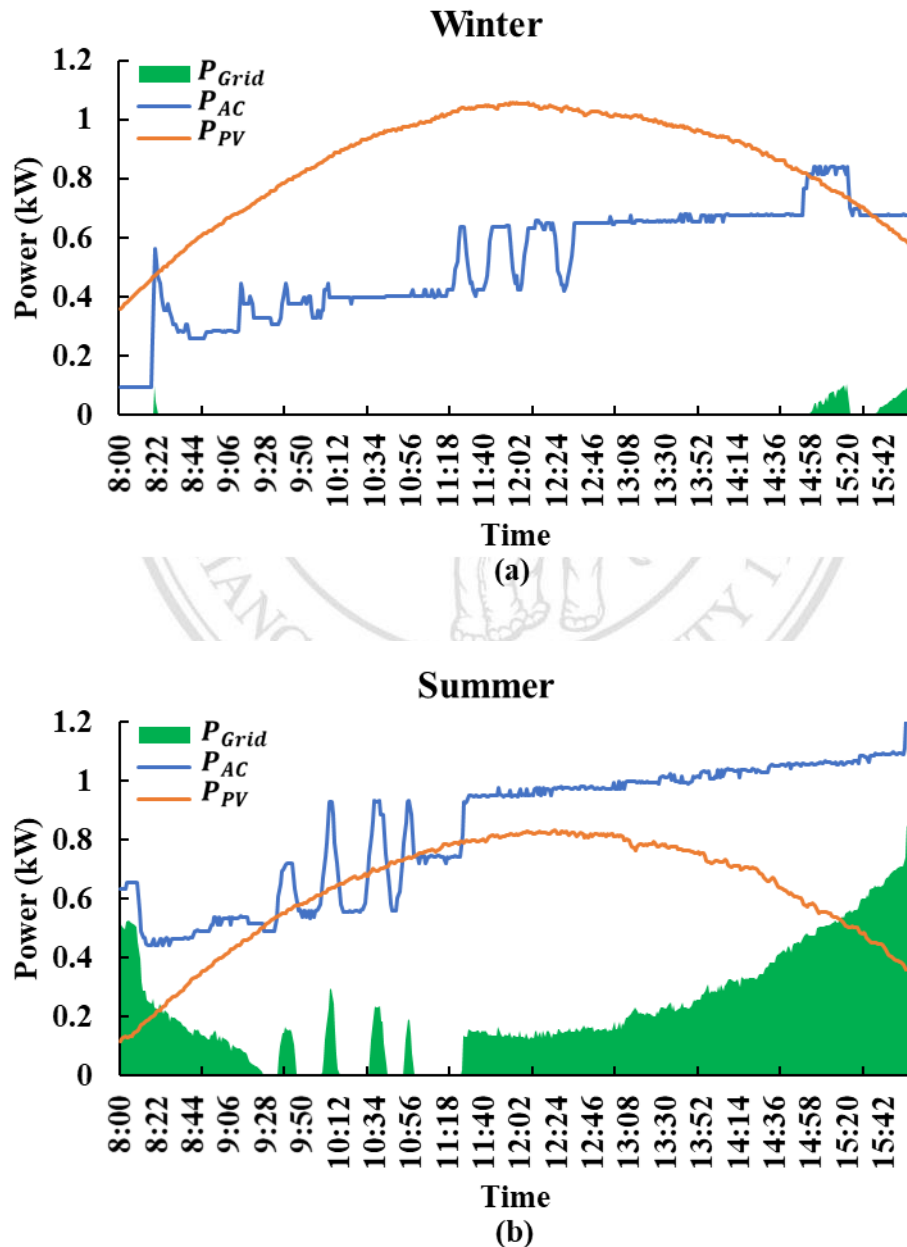


Figure 6.4 Electrical power reduction from grid line by four PV modules to the air conditioner unit. (a) a day in winter. (b) a day in summer.

CHAPTER 7

Energy Saving of the PV-Air Conditioner Unit with Assisted PCM bed

Cool Storage

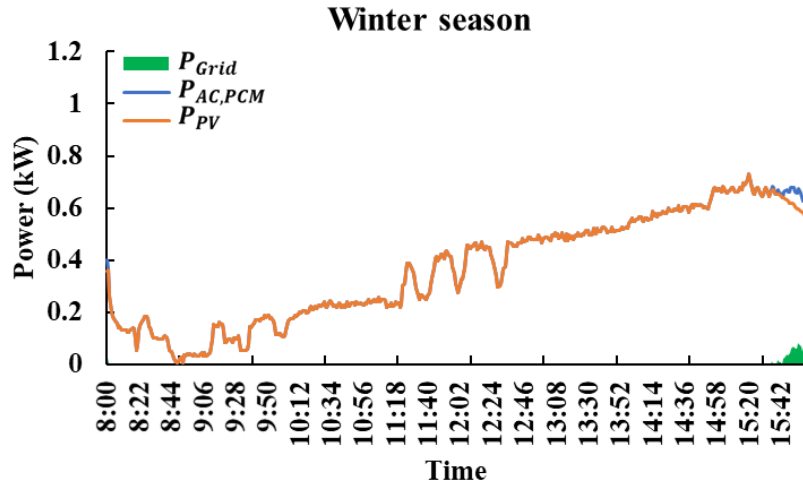
This chapter, the reduction of electrical power-consuming from grid line for the PV-air conditioner unit with assisted PCM packed bed cool storage and its economic analysis were carried out.

7.1 PV Modules Power Generation for the Air Conditioner with Assisted PCM Bed

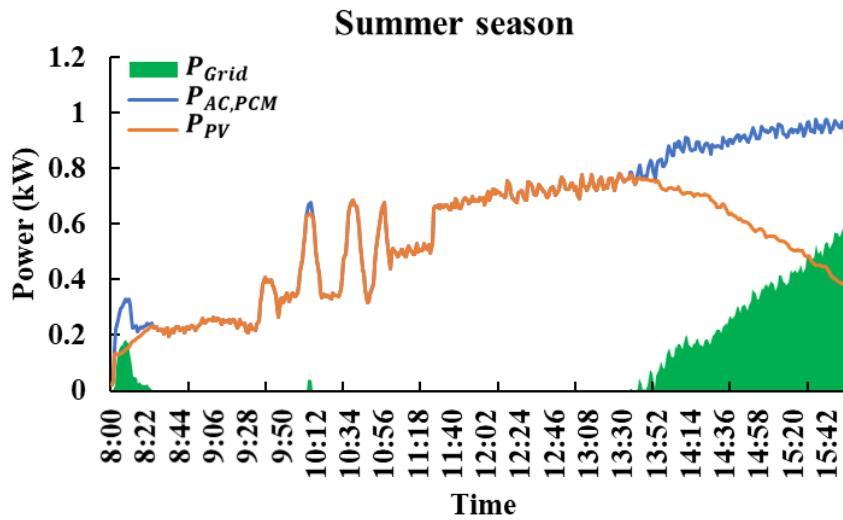
Cool Storage

Figures 7.1 (a, b) illustrates the electrical power requirement of air conditioner with PCM bed, useful power of PV modules to air conditioner, and the electrical power needed from grid line. The electrical power requirement of the air conditioner summer was higher than the winter season due to high ambient temperature. The PV module power generation could be matched and almost covered to the air conditioner unit with assisted PCM bed in winter due to high solar radiation. The results showed that the electrical power from grid line could be reduced around 99.44% and 84.62% in winter and summer, respectively.

ลิขสิทธิ์มหาวิทยาลัยเชียงใหม่
Copyright © by Chiang Mai University
All rights reserved



(a)



(b)

Figure 7.1 Electrical power reduction from grid line by four PV modules to air conditioner unit with assisted PCM bed. (a) a day in winter. (b) a day in summer.

7.2 Long Term Analysis of the PV-Air Conditioner Unit with Assisted PCM Bed Cool Storage

Due the cooling load of the air conditioner in each month did not exist, thus the average electrical power load of air conditioner with assisted PCM bed between winter and summer was considered in economic analysis to select the optimum number of PV module.

The optimum number of PV module could be determined at the lowest present worth of expense from the total investment cost, the electricity cost from the grid line, the maintenance cost and the salvage value. In this study, the unit cost of the solar module with the installation was 30 baht/Wp or 9,600 baht per module, 3% and 10% of the initial cost for the maintenance cost and the salvage value, respectively were taken for the calculation and 6.25% annual discount rate for 25 years of service. The unit cost of grid electricity was 5.78 baht/kWh.

Figure 7.2 shows the optimum numbers of PV modules at the lowest total expenses for the air conditioner unit with assisted PCM bed which the value was 3 modules with the payback period 8.92 years as shown in Figure 7.3

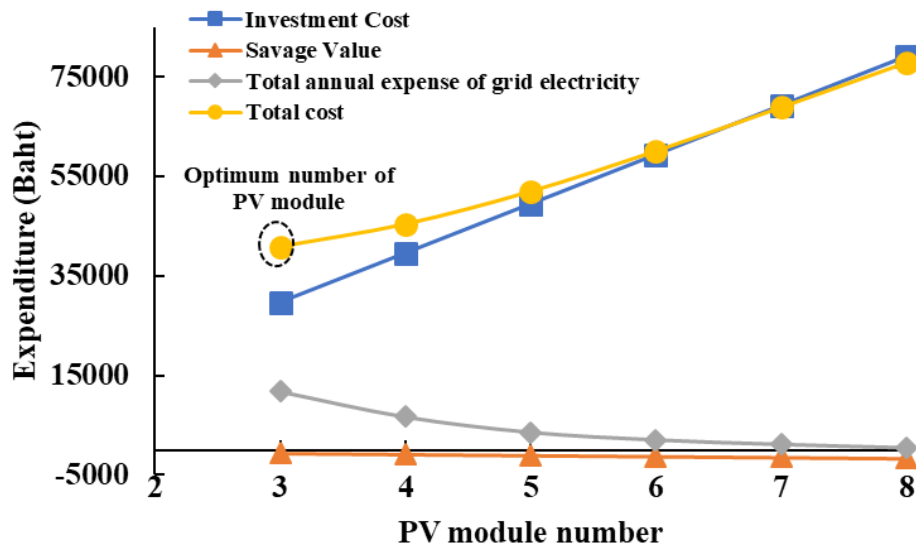


Figure 7.2 Optimum number of the PV-air conditioner with assisted PCM bed.

สงวนลิขสิทธิ์ © โดย Chiang Mai University
All rights reserved

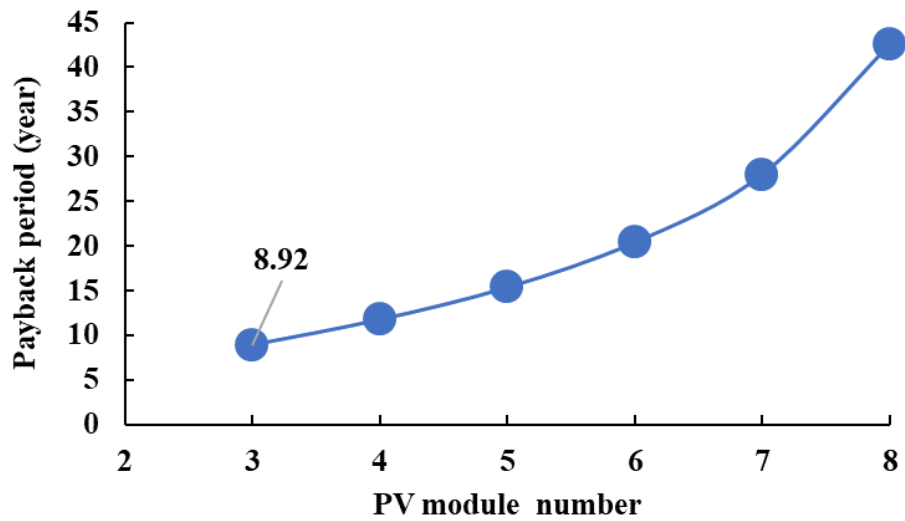
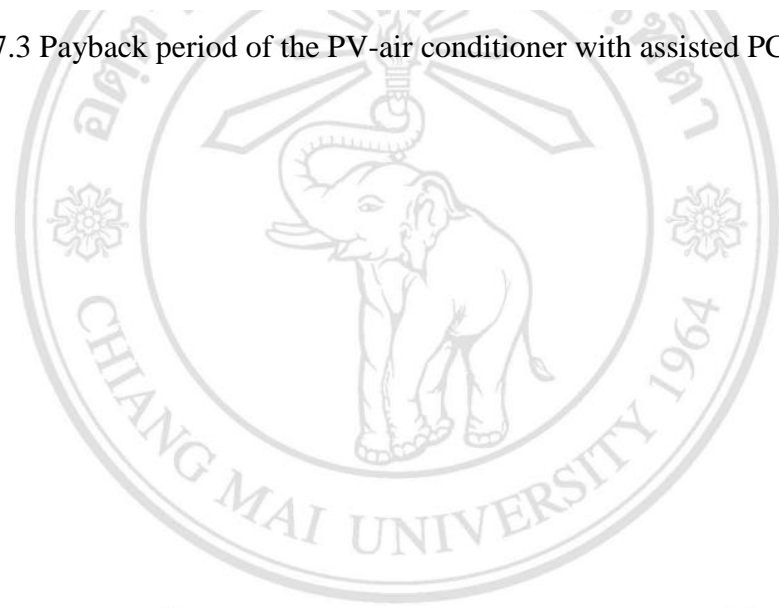


Figure 7.3 Payback period of the PV-air conditioner with assisted PCM bed.



ลิขสิทธิ์มหาวิทยาลัยเชียงใหม่
 Copyright© by Chiang Mai University
 All rights reserved

CHAPTER 8

Conclusions

- The energy cool storage RT-18 HC PCM packed bed having a melting point around 18 °C was studied the characteristic behaviors both charging and discharging periods. The mathematical model using the enthalpy method can be used based on the experimental data and simulation data showed good agreement with mean absolute percentage error (MAPE) less than 10%. Correlations of dimensionless operating parameter were significantly used in predicting the outlet air temperature at specific time in charging and discharging periods of the packed bed. A given values of the air mass flow rate, the inlet air temperature, the bed dimension, the PCM and air properties were considered.
- The appropriate thickness of PCM bed was 0.24 m. The evaluation of PCM energy cool storage in a reduction of energy consumption for air conditioner revealed that savings in the electrical energy consumption were 13.84% and 16.13% in winter and summer, respectively.
- Selection of appropriate number of 320 Wp polycrystalline PV modules in a reduction of grid power for air conditioner with PCM bed assisted in Chiang Mai was found out. The optimum number and the payback period of the PV-air conditioner with assisted PCM bed were 3 modules and 8.92 years, respectively.

ลิขสิทธิ์ © by Chiang Mai University
All rights reserved

REFERENCES

- [1] “August: Air conditioning demand set to grow rapidly over the coming decades.” [Online]. Available: <https://www.iea.org/newsroom/news/2016/august/air-conditioning-demand-set-to-grow-rapidly-over-the-coming-decades.html>. [Accessed: 09-Nov-2017].
- [2] “German International Cooperation Based in Bangkok - Topics.” [Online]. Available: <http://www.thai-german-cooperation.info/project/content/116>. [Accessed: 09-Nov-2017].
- [3] “Use of Phase Change Material as Thermal Buffer for Indoor Comfort - Nexus Energy Center.” [Online]. Available: <http://www.nexusenergycenter.org/use-phase-change-material-thermal-buffer-indoor-comfort/>. [Accessed: 19-Jun-2019].
- [4] F. J. Aguilera, P. V. Quilesa, and S. Aledob, “Operation and Energy Efficiency of a Hybrid Air Conditioner Simultaneously Connected to the Grid and to Photovoltaic Panels,” *Energy Procedia*, vol. 48, pp. 768–777, 2014.
- [5] D. Parker and J. Dunlop, “Solar Photovoltaic Air Conditioning of Residential Buildings,” *Florida Sol. Energy Cent.*, 1994.
- [6] K. S. Al Qdah, “Performance of Solar-Powered Air Conditioning System... - Google Scholar,” *Sci. Res. Publ.*, vol. 6, no. Smart Grid and renewable Energy, pp. 209–219, 2015.
- [7] S. Loem and T. Deethayat, “OPTIMUM NUMBER OF SOLAR CELL MODULES WITH AND WITHOUT PHASE CHANGE MATERIAL COOLING FOR AIR-CONDITIONING,” 2018.
- [8] D. Zhao and G. Tan, “Numerical analysis of a shell-and-tube latent heat storage unit with fins for air-conditioning application,” *Appl. Energy*, vol. 138, pp. 381–392, 2015.
- [9] A. H. Mosaffa and L. G. Farshi, “Exergoeconomic and environmental analyses of an air conditioning system using thermal energy storage,” *Appl. Energy*, vol. 162,

pp. 515–526, 2016.

- [10] M. Yamaha and S. Misaki, “The Evaluation of Peak Shaving by a Thermal Storage System Using Phase-Change Materials in Air Distribution Systems,” *HVAC&R Res.*, vol. 12, pp. 861–869, Sep. 2006.
- [11] C. Arkar and S. Medved, “Free cooling of a building using PCM heat storage integrated into the ventilation system,” *Sol. Energy*, vol. 81, no. 9, pp. 1078–1087, 2007.
- [12] S. Medved and C. Arkar, “Correlation between the local climate and the free-cooling potential of latent heat storage,” *Energy Build.*, vol. 40, no. 4, pp. 429–437, 2008.
- [13] C. Arkar, B. Vidrih, and S. Medved, “Efficiency of free cooling using latent heat storage integrated into the ventilation system of a low energy building,” *Int. J. Refrig.*, vol. 30, no. 1, pp. 134–143, 2007.
- [14] N. Chaiyat and T. Kiatsiriroat, “Energy reduction of building air-conditioner with phase change material in Thailand,” *Case Stud. Therm. Eng.*, vol. 4, pp. 175–186, 2014.
- [15] G. O. G. Löf and R. W. Hawley, “Unsteady-State Heat Transfer between air and loose solids,” *Ind. Eng. Chem.*, vol. 40, no. 6, pp. 1061–1070, Jun. 1948.
- [16] C. Osterwald, “Translation of device performance measurements to reference conditions,” *nrel.gov*.
- [17] G. M. Masters, *Renewable and efficient electric power systems*. 2013.
- [18] “POWER Data Access Viewer.” [Online]. Available: <https://power.larc.nasa.gov/data-access-viewer/>. [Accessed: 08-Mar-2019].
- [19] “Air-Conditioner from Solar Cell - PAC SolarAire.” [Online]. Available: <http://www.pac.co.th/en/all-products/pac-solaraire/>. [Accessed: 19-Jun-2019].
- [20] “solar cell - Google Search.” [Online]. Available: https://www.google.co.th/search?biw=1366&bih=633&tbm=isch&q=solar+cell&backchip=g_1:photovoltaic&chips=q:solar+cell,g_1:pv+solar&sa=X&ved=0ahUKEWjO77n_98zXAhULRo8KHRz2BQAQ4VYIIigB#imgrc=6r7DvNWW1JkpD

- M: [Accessed: 20-Nov-2017].
- [21] “MS-602 Pyranometer | EKO Instruments.” [Online]. Available: <https://eko-eu.com/products/solar-energy/pyranometers/ms-602-pyranometer>. [Accessed: 21-Feb-2019].
- [22] “K Type Thermocouple Compensation Wire, Compensation Cable - Buy Thermocouple Cables K Type, Thermocouple Cables, K Type Thermocouple Wire Product on Alibaba.com.” [Online]. Available: https://www.alibaba.com/product-detail/K-type-thermocouple-compensation-wire-compensation_60596611075.html?spm=a2700.7724838.2017115.96.4ca76a6f4io tq8&s=p. [Accessed: 20-Feb-2018].
- [23] “Data Loggers, Hygrometers, Therometers, Transmitters - HUATO, A Professional Manufacturer.” [Online]. Available: http://www.huato.cn/s220_T8.html. [Accessed: 21-Nov-2017].
- [24] “[Chauvin Arnoux Metrix.” [Online]. Available: <http://www.chauvin-arnoux.com/en/produit/c-a-8220.html>. [Accessed: 26-Jun-2018].
- [25] “Chauvin Arnoux PAC 93.” [Online]. Available: <https://www.souz-pribor.ru/catalog/brands/?ID=Chauvin Arnoux>. [Accessed: 09-Jul-2018].
- [26] “hot wire anemometer am-4234sd HD - Google Search.” [Online]. Available: https://www.google.co.th/search?dcr=0&biw=1366&bih=633&tbm=isch&sa=1&ei=aN8TWvWxMcfmvgTV_6TABg&q=hot+wire+anemometer+am-4234sd+HD&oq=hot+wire+anemometer+am-4234sd+HD&gs_l=psy-ab.3...60068.61849.0.62601.3.3.0.0.0.0.383.496.0j1j0j1.2.0....0...1c.1.64.psy-ab. [Accessed: 21-Nov-2017].
- [27] C. Tantakitti, N. Rungpairojcharoen, Thutchai Tontanasarn, and S. Kaewjino, “Feasibility Study to Substitute the EER with the SEER – Case Study Chiang Mai, Thailand - Google Search,” 2012. [Online]. Available: <https://www.google.com/search?client=firefox-b-d&q=Feasibility+Study+to+Substitute+the+EER+with+the+SEER+-+Case+Study+Chiang+Mai%2C+Thailand>. [Accessed: 08-Feb-2019].



ลิขสิทธิ์มหาวิทยาลัยเชียงใหม่
Copyright© by Chiang Mai University
All rights reserved

APPENDIX A

Validation of the Bed Temperature and the Outlet Air Temperature of the Bed in Charging Period

A.1 Bed Temperature T_b (°C)

Time (min)	$T_{b,x=0.02m}$		$T_{b,x=0.06m}$		$T_{b,x=0.10m}$		$T_{b,x=0.14m}$		$T_{b,x=0.18m}$		$T_{b,x=0.22m}$	
	Exp	Sim										
1	23	23.1	23.9	23.6	23.0	24.0	23.6	24.3	24.4	24.5	24.5	24.7
3	19.72	19.7	23.7	21.1	19.7	22.2	23.5	22.9	23.0	23.5	23.5	23.9
5	18	18.0	22.2	18.9	18.0	20.4	22.6	21.5	21.6	22.4	22.8	23.0
7	18	18.0	20.0	18.0	18.0	18.8	21.0	20.2	20.3	21.3	22.0	22.1
9	17.9	18.0	18.4	18.0	17.9	18.0	19.4	19.0	18.9	20.2	20.5	21.2
11	17.9	18.0	17.8	18.0	17.9	18.0	18.4	18.0	18.4	19.2	19.5	20.3
13	17.9	18.0	17.8	18.0	17.9	18.0	18.0	18.0	18.3	18.4	19.0	19.5
15	17.9	18.0	17.9	18.0	17.9	18.0	18.0	18.0	18.2	18.0	18.0	18.9
17	18	18.0	18.0	18.0	18.0	18.0	18.1	18.0	18.2	18.0	18.0	18.3
19	17.9	18.0	18.0	18.0	17.9	18.0	18.0	18.0	18.2	18.0	17.9	18.0
29	18	18.0	18.1	18.0	18.0	18.0	18.1	18.0	18.1	18.0	18.0	18.0
39	18.1	18.0	18.3	18.0	18.1	18.0	18.2	18.0	18.2	18.0	18.1	18.0
49	18.1	18.0	18.3	18.0	18.0	18.0	18.2	18.0	18.2	18.0	18.0	18.0
59	17.4	18.0	18.2	18.0	17.9	18.0	18.3	18.0	18.2	18.0	17.9	18.0
69	10.8	9.5	18.0	18.0	18.1	18.0	18.1	18.0	18.2	18.0	18.1	18.0
79	6.1	5.8	17.5	18.0	18.1	18.0	18.0	18.0	18.2	18.0	18.1	18.0
89	5.3	5.1	12.8	10.5	18.1	18.0	18.0	18.0	18.2	18.0	18.1	18.0
99	5.3	5.0	6.4	6.0	18.0	18.0	17.8	18.0	18.1	18.0	17.9	18.0
109	5	5.0	5.5	5.2	14.6	11.5	17.9	18.0	18.1	18.0	17.9	18.0
119	5.1	5.0	5.2	5.0	6.8	6.2	17.7	18.0	18.0	18.0	18.1	18.0
129	5.2	5.0	5.3	5.0	5.5	5.2	13.6	12.7	18.0	18.0	18.1	18.0
139	5	5.0	5.1	5.0	5.3	5.0	6.6	6.4	18.0	18.0	18.1	18.0
149	5.1	5.0	5.2	5.0	5.1	5.0	5.6	5.2	15.2	14.2	18.1	18.0
159	5.2	5.0	5.3	5.0	5.1	5.0	5.4	5.0	7.1	6.6	18.1	18.0

A.1 Bed Temperature T_b (°C) (continued)

Time (min)	$T_{b,x=0.02m}$		$T_{b,x=0.06m}$		$T_{b,x=0.10m}$		$T_{b,x=0.14m}$		$T_{b,x=0.18m}$		$T_{b,x=0.22m}$	
	Exp	Sim										
169	5.2	5.0	5.3	5.0	5.2	5.0	5.3	5.0	5.6	5.3	16.3	15.9
179	5.1	5.0	5.2	5.0	5.2	5.0	5.3	5.0	5.3	5.0	8.0	6.9
189	5.1	5.0	5.2	5.0	5.1	5.0	5.2	5.0	5.0	5.0	5.7	5.3
199	5.2	5.0	5.3	5.0	5.2	5.0	5.3	5.0	5.2	5.0	5.4	5.1
209	5.2	5.0	5.3	5.0	5.2	5.0	5.3	5.0	5.2	5.0	5.0	5.0
219	5.1	5.0	5.2	5.0	5.2	5.0	5.1	5.0	5.2	5.0	5.1	5.0
229	5.2	5.0	5.3	5.0	5.1	5.0	5.3	5.0	5.0	5.0	5.2	5.0
239	5.2	5.0	5.3	5.0	5.2	5.0	5.3	5.0	5.1	5.0	5.2	5.0
249	5.2	5.0	5.3	5.0	5.2	5.0	5.3	5.0	5.2	5.0	5.1	5.0

A.1 Outlet Air Temperature T_a (°C)

Time (min)	$T_{a,x=0.04m}$		$T_{a,x=0.08m}$		$T_{a,x=0.12m}$		$T_{a,x=0.16m}$		$T_{a,x=0.20m}$		$T_{a,x=0.24m}$	
	Exp	Sim										
1	12.0	10.3	15.4	14.7	17.9	17.7	19.5	19.9	22.6	21.4	23.6	22.5
5	8.9	8.6	13.0	11.9	15.4	14.7	17.0	16.9	19.0	18.7	21.1	20.1
9	8.7	8.5	11.7	11.3	14.0	13.3	15.6	15.2	17.0	16.8	18.9	18.2
13	8.7	8.5	11.6	11.3	13.9	13.3	15.4	14.7	16.5	15.9	18.0	17.1
17	8.8	8.5	11.6	11.3	13.7	13.3	15.3	14.7	16.4	15.7	17.4	16.5
21	8.5	8.5	11.6	11.3	13.7	13.3	15.3	14.7	16.4	15.7	17.0	16.4
25	8.4	8.5	11.5	11.3	13.7	13.3	15.2	14.7	16.3	15.7	16.9	16.4
29	8.3	8.5	11.2	11.3	13.6	13.3	15.1	14.7	16.2	15.7	16.8	16.4
33	8.4	8.5	11.3	11.3	13.5	13.3	15.0	14.7	16.1	15.7	16.8	16.4
37	8.3	8.5	11.3	11.3	13.4	13.3	14.9	14.7	16.0	15.7	16.5	16.4
41	8.2	8.5	11.1	11.3	13.3	13.3	14.8	14.7	15.9	15.7	16.6	16.4
45	8.2	8.5	11.1	11.3	13.2	13.3	14.7	14.7	15.8	15.7	16.2	16.4
49	8.2	8.5	11.1	11.3	13.0	13.3	14.5	14.7	15.6	15.7	16.4	16.4
53	7.9	8.5	10.6	11.3	12.9	13.3	14.8	14.7	15.5	15.7	16.3	16.4
57	7.7	8.5	10.5	11.3	12.9	13.3	14.3	14.7	15.4	15.7	16.2	16.4
61	7.6	8.1	10.2	11.0	12.5	13.1	14.6	14.6	15.4	15.6	16.2	16.3
65	7.2	7.5	9.9	10.6	12.4	12.8	14.1	14.4	15.4	15.4	16.2	16.2
69	6.8	6.9	9.6	10.2	12.0	12.5	13.8	14.1	15.2	15.3	16.0	16.1
73	6.5	6.2	9.2	9.7	11.8	12.2	13.5	13.9	15.1	15.1	15.9	16.0
77	6.1	5.6	8.9	9.2	11.4	11.8	13.2	13.6	15.1	14.9	15.9	15.8
81	5.8	5.3	8.3	8.5	10.7	11.3	12.8	13.3	14.7	14.7	15.5	15.7
85	5.6	5.1	7.6	7.9	10.4	10.9	12.5	13.0	14.5	14.5	15.5	15.5
89	5.2	5.1	6.8	7.2	9.9	10.4	11.9	12.6	14.1	14.2	15.1	15.4
93	5.1	5.0	6.0	6.5	9.3	9.9	11.7	12.3	13.7	14.0	15.1	15.2
97	5.1	5.0	5.2	5.7	8.5	9.3	11.3	11.9	13.3	13.7	15.1	15.0
101	5.0	5.0	5.2	5.4	8.0	8.7	10.9	11.5	13.1	13.4	14.7	14.8
105	5.1	5.0	5.2	5.2	7.7	8.1	10.5	11.0	12.7	13.1	14.7	14.5
109	5.1	5.0	5.1	5.1	7.1	7.4	10.1	10.5	12.4	12.8	14.3	14.3
113	5.2	5.0	5.1	5.0	6.6	6.7	9.5	10.0	12.0	12.4	13.9	14.1

A.1 Outlet Air Temperature T_a (°C) (continued)

Time (min)	$T_{a,x=0.04m}$		$T_{a,x=0.08m}$		$T_{a,x=0.12m}$		$T_{a,x=0.16m}$		$T_{a,x=0.20m}$		$T_{a,x=0.24m}$	
	Exp	Sim	Exp	Sim								
117	5.2	5.0	5.0	5.0	6.2	5.9	9.0	9.5	11.6	12.0	13.5	13.8
121	5.2	5.0	5.1	5.0	6.0	5.4	8.2	8.8	11.2	11.6	13.1	13.5
125	5.2	5.0	5.1	5.0	5.7	5.2	8.1	8.2	10.8	11.1	12.7	13.2
129	5.2	5.0	5.2	5.0	5.4	5.1	7.0	7.5	10.4	10.6	12.3	12.8
133	5.0	5.0	5.2	5.0	5.2	5.1	6.3	6.8	10.0	10.1	11.9	12.5
137	5.1	5.0	5.2	5.0	5.0	5.0	5.8	6.0	9.4	9.6	11.5	12.1
141	5.1	5.0	5.2	5.0	5.1	5.0	5.4	5.5	8.7	9.0	11.1	11.7
145	5.0	5.0	5.2	5.0	5.2	5.0	5.2	5.2	8.3	8.4	10.8	11.2
149	5.1	5.0	5.0	5.0	5.2	5.0	4.9	5.1	7.7	7.7	10.4	10.7
153	5.1	5.0	5.1	5.0	5.2	5.0	5.2	5.1	7.0	7.0	9.8	10.3
157	5.2	5.0	5.2	5.0	5.2	5.0	5.2	5.0	6.1	6.2	9.4	9.7
161	5.2	5.0	5.2	5.0	5.0	5.0	5.0	5.0	5.5	5.6	8.9	9.1
165	5.2	5.0	5.2	5.0	5.1	5.0	5.1	5.0	5.5	5.3	8.2	8.4
169	5.2	5.0	5.2	5.0	5.0	5.0	5.0	5.0	5.3	5.1	7.7	7.8
173	5.2	5.0	5.2	5.0	5.0	5.0	5.0	5.0	5.3	5.1	7.1	7.1
177	5.0	5.0	5.0	5.0	5.1	5.0	5.1	5.0	5.3	5.0	6.2	6.3
181	5.1	5.0	5.1	5.0	5.1	5.0	5.1	5.0	5.4	5.0	5.2	5.6
185	5.1	5.0	5.1	5.0	5.1	5.0	5.1	5.0	5.4	5.0	5.2	5.3
189	5.0	5.0	5.0	5.0	5.2	5.0	5.2	5.0	5.4	5.0	5.2	5.2
193	5.1	5.0	5.1	5.0	5.2	5.0	5.2	5.0	5.4	5.0	4.9	5.1
197	5.1	5.0	5.1	5.0	5.2	5.0	5.2	5.0	5.2	5.0	4.7	5.0
206	5.2	5.0	5.2	5.0	5.0	5.0	5.0	5.0	5.0	5.0	4.8	5.0
215	5.2	5.0	5.2	5.0	5.1	5.0	5.1	5.0	5.1	5.0	4.9	5.0
224	5.2	5.0	5.2	5.0	5.2	5.0	5.2	5.0	5.2	5.0	4.9	5.0
233	5.0	5.0	5.0	5.0	5.2	5.0	5.2	5.0	5.2	5.0	4.9	5.0
242	5.2	5.0	5.2	5.0	5.2	5.0	5.2	5.0	5.0	5.0	4.7	5.0

APPENDIX B

Validation of the Bed Temperature and the Outlet Air Temperature of the Bed in Discharging Period

B.1 Bed Temperature T_b (°C)

Time (min)	$T_{b,x=0.02m}$		$T_{b,x=0.06m}$		$T_{b,x=0.10m}$		$T_{b,x=0.14m}$		$T_{b,x=0.18m}$		$T_{b,x=0.22m}$	
	Exp	Sim										
1	11.0	7.2	7.2	6.5	11.0	6.0	7.3	5.7	10.5	5.5	6.6	5.3
5	13.8	13.7	9.4	11.5	13.8	9.9	9.5	8.6	10.3	7.7	7.4	7.0
9	15.2	17.9	12.2	15.4	15.2	13.3	12.3	11.6	11.3	10.2	8.2	9.1
19	16.5	18.0	15.8	18.0	16.5	18.0	15.9	17.1	14.3	15.6	12.2	14.2
29	17.1	18.0	16.8	18.0	17.1	18.0	16.9	18.0	15.8	18.0	15.8	17.3
39	17.4	18.0	17.3	18.0	17.4	18.0	17.4	18.0	16.5	18.0	16.8	18.0
49	17.7	18.0	17.6	18.0	17.7	18.0	17.7	18.0	16.7	18.0	17.3	18.0
59	17.8	18.0	17.6	18.0	17.7	18.0	17.8	18.0	16.9	18.0	17.6	18.0
69	17.9	18.0	17.8	18.0	17.7	18.0	17.8	18.0	17.1	18.0	17.6	18.0
79	18.0	18.0	17.8	18.0	17.8	18.0	17.9	18.0	17.2	18.0	17.8	18.0
89	18.0	18.0	17.8	18.0	17.9	18.0	17.8	18.0	17.2	18.0	17.8	18.0
99	18.1	18.0	17.9	18.0	18.0	18.0	17.9	18.0	17.3	18.0	18.0	18.0
109	18.4	18.0	18.0	18.0	17.9	18.0	18.0	18.0	17.3	18.0	18.0	18.0
119	18.3	18.0	18.1	18.0	18.0	18.0	18.1	18.0	17.3	18.0	17.9	18.0
129	18.5	18.0	18.1	18.0	18.2	18.0	18.1	18.0	17.3	18.0	17.9	18.0
139	19.2	18.0	18.2	18.0	18.2	18.0	18.2	18.0	17.4	18.0	18.0	18.0
149	21.1	21.7	18.1	18.0	18.3	18.0	18.1	18.0	17.5	18.0	17.9	18.0
159	23.4	23.9	18.3	18.0	18.3	18.0	18.1	18.0	17.4	18.0	18.0	18.0
169	24.3	24.6	18.3	18.0	18.3	18.0	18.3	18.0	17.5	18.0	18.0	18.0
179	25.0	24.9	18.5	18.0	18.6	18.0	18.5	18.0	17.6	18.0	18.0	18.0
189	25.3	25.0	19.4	18.0	18.7	18.0	18.6	18.0	17.8	18.0	18.1	18.0
199	25.3	25.0	21.3	22.0	18.8	18.0	18.6	18.0	17.8	18.0	18.1	18.0
209	25.3	25.0	23.3	24.0	18.8	18.0	18.7	18.0	17.8	18.0	18.1	18.0

B.1 Bed Temperature T_b (°C) (continued)

Time (min)	$T_{b,x=0.02m}$		$T_{b,x=0.06m}$		$T_{b,x=0.10m}$		$T_{b,x=0.14m}$		$T_{b,x=0.18m}$		$T_{b,x=0.22m}$	
	Exp	Sim										
219	25.2	25.0	24.4	24.7	18.8	18.0	18.7	18.0	17.8	18.0	18.1	18.0
229	25.2	25.0	25.0	24.9	19.3	18.0	18.8	18.0	17.8	18.0	18.1	18.0
239	25.2	25.0	25.3	25.0	20.1	18.0	18.6	18.0	18.0	18.0	18.1	18.0
249	25.3	25.0	25.3	25.0	22.5	22.6	18.6	18.0	18.0	18.0	18.2	18.0
259	25.3	25.0	25.3	25.0	23.9	24.2	18.5	18.0	17.9	18.0	18.0	18.0
269	25.3	25.0	25.3	25.0	24.7	24.7	18.6	18.0	18.0	18.0	18.0	18.0
279	25.3	25.0	25.3	25.0	25.2	24.9	18.8	18.0	18.0	18.0	18.0	18.0
289	25.4	25.0	25.4	25.0	25.4	25.0	20.0	19.4	18.1	18.0	18.1	18.0
299	25.3	25.0	25.3	25.0	25.3	25.0	22.2	23.1	18.2	18.0	18.1	18.0
309	25.4	25.0	25.4	25.0	25.2	25.0	23.6	24.3	18.4	18.0	18.2	18.0
319	25.3	25.0	25.3	25.0	25.2	25.0	24.8	24.8	18.4	18.0	18.3	18.0
329	25.4	25.0	25.3	25.0	25.2	25.0	25.3	24.9	18.6	18.0	18.2	18.0
339	25.4	25.0	25.3	25.0	25.3	25.0	25.4	25.0	19.8	20.4	18.1	18.0
349	25.2	25.0	25.2	25.0	25.3	25.0	25.5	25.0	22.0	23.4	18.2	18.0
359	25.2	25.0	25.2	25.0	25.3	25.0	25.5	25.0	23.7	24.5	18.1	18.0
369	25.2	25.0	25.2	25.0	25.3	25.0	25.6	25.0	24.6	24.8	18.6	18.0
379	25.3	25.0	25.3	25.0	25.4	25.0	25.5	25.0	25.1	24.9	18.8	18.0
389	25.3	25.0	25.3	25.0	25.4	25.0	25.5	25.0	25.4	25.0	20.0	21.7
399	25.3	25.0	25.3	25.0	25.3	25.0	25.5	25.0	25.3	25.0	22.2	23.9
409	25.3	25.0	25.3	25.0	25.3	25.0	25.5	25.0	25.0	25.0	23.5	24.6
419	25.4	25.0	25.4	25.0	25.3	25.0	25.5	25.0	25.2	25.0	25.1	24.9
429	25.3	25.0	25.3	25.0	25.3	25.0	25.6	25.0	25.2	25.0	25.3	25.0
439	25.4	25.0	25.4	25.0	25.2	25.0	25.2	25.0	25.2	25.0	25.4	25.0
449	25.3	25.0	25.3	25.0	25.2	25.0	25.4	25.0	25.3	25.0	25.5	25.0
459	25.4	25.0	25.3	25.0	25.2	25.0	25.4	25.0	25.3	25.0	25.5	25.0
469	25.4	25.0	25.3	25.0	25.3	25.0	25.4	25.0	25.4	25.0	25.6	25.0
479	25.2	25.0	25.2	25.0	25.3	25.0	25.5	25.0	25.3	25.0	25.5	25.0
489	25.2	25.0	25.2	25.0	25.3	25.0	25.5	25.0	25.3	25.0	25.5	25.0
499	25.2	25.0	25.2	25.0	25.3	25.0	25.6	25.0	25.3	25.0	25.5	25.0

B.2 Outlet Air Temperature T_a (°C)

Time (min)	$T_{a,x=0.04m}$		$T_{a,x=0.08m}$		$T_{a,x=0.12m}$		$T_{a,x=0.16m}$		$T_{a,x=0.20m}$		$T_{a,x=0.24m}$	
	Exp	Sim										
1	8.2	19.3	6.7	14.8	5.6	11.7	5.1	9.6	8.8	8.1	4.6	7.1
5	19.7	21.4	15.6	17.9	15.4	15.1	14.7	12.8	14.9	11.0	13.4	9.6
9	21.2	22.7	18.2	20.2	17.6	17.7	16.7	15.6	16.3	13.7	16.0	12.1
13	22.6	23.0	19.5	21.3	19.1	19.4	17.8	17.6	17.1	15.9	17.4	14.2
17	23.3	23.0	20.5	21.4	19.8	20.2	18.8	18.8	17.8	17.4	18.2	15.9
21	23.6	23.0	20.9	21.4	20.3	20.3	19.4	19.4	18.2	18.4	18.5	17.2
25	23.8	23.0	21.4	21.4	20.7	20.3	19.9	19.6	18.5	18.9	19.0	18.0
29	22.7	23.0	21.3	21.4	20.1	20.3	19.5	19.6	18.8	19.1	18.7	18.5
33	22.5	23.0	21.0	21.4	20.0	20.3	19.3	19.6	18.9	19.1	18.4	18.7
37	21.8	23.0	21.0	21.4	19.7	20.3	19.1	19.6	19.0	19.1	18.3	18.7
40	22.5	23.0	20.9	21.4	20.0	20.3	19.4	19.6	19.1	19.1	18.4	18.7
50	23.1	23.0	21.4	21.4	20.5	20.3	19.8	19.6	19.3	19.1	18.8	18.7
60	22.9	23.0	21.4	21.4	20.5	20.3	19.8	19.6	19.5	19.1	18.8	18.7
70	23.0	23.0	21.5	21.4	20.6	20.3	19.9	19.6	19.5	19.1	18.9	18.7
80	22.4	23.0	21.7	21.4	20.3	20.3	19.7	19.6	19.6	19.1	19.1	18.7
90	23.5	23.0	21.6	21.4	21.0	20.3	20.2	19.6	19.6	19.1	19.1	18.7
100	23.3	23.0	21.8	21.4	21.0	20.3	20.1	19.6	19.7	19.1	19.2	18.7
110	22.6	23.0	21.5	21.4	20.5	20.3	19.8	19.6	19.7	19.1	19.0	18.7
120	22.9	23.0	21.8	21.4	20.8	20.3	20.1	19.6	19.7	19.1	19.2	18.7
130	22.6	23.1	21.6	21.5	20.6	20.4	19.9	19.6	19.7	19.1	19.0	18.8
140	23.0	23.5	22.0	21.7	21.0	20.5	20.3	19.7	19.8	19.2	19.4	18.8
150	23.7	23.9	22.4	22.0	21.0	20.7	20.2	19.9	19.8	19.3	19.3	18.9
160	24.2	24.3	22.9	22.3	21.1	21.0	20.2	20.0	19.8	19.4	19.3	18.9
170	24.7	24.8	23.4	22.7	21.2	21.2	20.5	20.2	19.8	19.5	19.4	19.0
180	24.6	24.9	23.5	23.0	21.5	21.4	20.4	20.3	19.8	19.6	19.4	19.1
190	25.2	25.0	23.9	23.4	21.4	21.7	20.7	20.5	19.9	19.7	19.4	19.2
200	24.7	25.0	24.3	23.9	21.5	22.0	21.0	20.8	19.8	19.9	19.6	19.3
210	25.0	25.0	24.7	24.4	22.1	22.3	21.1	21.0	20.0	20.0	19.9	19.4
220	25.3	25.0	24.8	24.8	22.2	22.7	21.5	21.2	19.9	20.2	19.8	19.5

B.2 Outlet Air Temperature T_a (°C) (continued)

Time (min)	$T_{a,x=0.04m}$		$T_{a,x=0.08m}$		$T_{a,x=0.12m}$		$T_{a,x=0.16m}$		$T_{a,x=0.20m}$		$T_{a,x=0.24m}$	
	Exp	Sim										
230	25.2	25.0	24.9	24.9	22.8	23.1	21.8	21.5	19.9	20.4	20.2	19.6
240	25.1	25.0	25.2	25.0	23.2	23.5	22.1	21.8	20.0	20.6	20.2	19.8
250	25.0	25.0	25.4	25.0	23.8	24.0	22.2	22.1	20.0	20.8	20.6	19.9
260	25.1	25.0	25.1	25.0	23.4	24.5	23.0	22.4	20.0	21.0	20.3	20.1
270	25.3	25.0	25.2	25.0	24.6	24.8	23.1	22.8	20.4	21.3	20.6	20.2
280	25.5	25.0	25.2	25.0	24.2	24.9	23.2	23.2	21.1	21.5	20.6	20.4
290	25.0	25.0	25.2	25.0	24.6	25.0	23.4	23.6	21.2	21.8	20.7	20.6
300	25.3	25.0	25.3	25.0	24.2	25.0	23.7	24.1	21.9	22.1	20.8	20.8
310	24.8	25.0	25.3	25.0	24.3	25.0	24.0	24.6	22.3	22.5	20.9	21.1
320	24.5	25.0	25.4	25.0	24.2	25.0	24.3	24.9	22.5	22.9	21.0	21.3
330	24.8	25.0	25.3	25.0	24.5	25.0	24.4	25.0	22.8	23.3	21.2	21.6
340	24.4	25.0	25.4	25.0	24.6	25.0	24.2	25.0	23.2	23.7	21.4	21.9
350	24.7	25.0	25.3	25.0	24.9	25.0	24.3	25.0	23.5	24.2	21.7	22.2
360	25.1	25.0	25.4	25.0	25.2	25.0	24.3	25.0	24.2	24.7	22.8	22.6
370	25.5	25.0	25.3	25.0	25.1	25.0	24.3	25.0	24.7	24.9	23.4	22.9
380	25.2	25.0	25.4	25.0	24.8	25.0	24.5	25.0	24.9	25.0	23.4	23.4
390	24.8	25.0	25.1	25.0	25.0	25.0	24.5	25.0	25.2	25.0	23.7	23.8
400	25.1	25.0	25.2	25.0	25.1	25.0	24.6	25.0	25.3	25.0	23.9	24.3
410	25.8	25.0	25.2	25.0	24.9	25.0	24.5	25.0	25.3	25.0	24.2	24.8
420	25.3	25.0	25.4	25.0	25.0	25.0	24.7	25.0	25.3	25.0	24.4	24.9
430	25.5	25.0	25.4	25.0	25.0	25.0	24.9	25.0	25.4	25.0	24.6	25.0
440	25.5	25.0	25.2	25.0	25.3	25.0	24.8	25.0	25.4	25.0	24.8	25.0
450	25.5	25.0	25.2	25.0	25.3	25.0	25.3	25.0	25.3	25.0	24.6	25.0
460	25.5	25.0	25.2	25.0	25.2	25.0	25.2	25.0	25.3	25.0	24.8	25.0
470	25.5	25.0	25.3	25.0	25.5	25.0	25.5	25.0	25.3	25.0	25.1	25.0
480	25.5	25.0	25.3	25.0	25.5	25.0	25.5	25.0	25.3	25.0	25.0	25.0
490	25.5	25.0	25.3	25.0	25.7	25.0	25.7	25.0	25.2	25.0	25.1	25.0
500	25.5	25.0	25.3	25.0	25.7	25.0	25.7	25.0	25.2	25.0	25.2	25.0

APPENDIX C

C.1 Validation of PV Module Power Output

Time	I_T (W/m ²)	T_{amb} (°C)	T_c (°C)		P_{PV} (kW)	
			Exp	Sim	Exp	Sim
7:17	30	19.8	18.9	20.57	0.00	0.01
7:26	52	20.3	20.3	21.63	0.00	0.02
7:35	140	20.8	21	24.39	0.00	0.04
7:44	191	21.3	23.4	26.19	0.05	0.06
7:53	202	22	25.1	27.18	0.05	0.06
8:02	241	21.8	25.6	27.98	0.06	0.08
8:11	272	22.6	26.6	29.57	0.07	0.09
8:20	345	22.7	28.1	31.54	0.09	0.11
8:29	378	23	29.6	32.69	0.10	0.12
8:38	406	24.1	30.3	34.50	0.11	0.12
8:47	445	26.4	34.1	37.80	0.12	0.13
8:56	491	26	36.9	38.58	0.13	0.15
9:05	539	25.1	39.1	38.91	0.15	0.16
9:14	566	26.4	41.3	40.90	0.16	0.17
9:23	595	26.7	42.2	41.95	0.17	0.18
9:32	626	27.7	44	43.74	0.18	0.18
9:41	661	27.7	45.1	44.64	0.19	0.19
9:50	686	27.8	45.8	45.38	0.19	0.20
9:59	710	28.9	46.8	47.09	0.20	0.21
10:08	735	29.5	48.1	48.33	0.21	0.21

C.1 Validation of PV Module Power Output (continued)

Time	I_T (W/m ²)	T_{amb} (°C)	T_c (°C)		P_{PV} (kW)	
			Exp	Sim	Exp	Sim
10:17	756	30.2	47.6	49.57	0.22	0.22
10:26	780	30.2	47.8	50.19	0.22	0.22
10:35	804	31.3	49.5	51.90	0.23	0.23
10:44	821	30.1	49.5	51.14	0.24	0.23
10:53	851	31	51.3	52.81	0.24	0.24
11:09	904	31.3	50.2	54.47	0.28	0.25
11:18	881	33.3	53.7	55.88	0.25	0.25
11:27	894	32.7	55.2	55.61	0.25	0.25
11:36	903	33.2	56.8	56.34	0.25	0.25
11:45	906	32.5	57.2	55.72	0.25	0.25
11:54	896	33.1	57.1	56.06	0.25	0.25
12:03	902	34	57.3	57.11	0.25	0.25
12:12	905	32.1	56.1	55.29	0.25	0.25
12:21	897	31.9	57.1	54.89	0.25	0.25
12:30	913	33.7	58	57.10	0.25	0.25
12:39	863	31.5	57.5	53.61	0.24	0.24
12:48	869	33	57.5	55.27	0.24	0.24
13:00	883	33	55.5	55.63	0.25	0.25
13:09	925	34.1	57.7	57.80	0.26	0.26
13:18	957	33.6	59.4	58.12	0.26	0.26
13:27	888	31.8	56.2	54.56	0.25	0.25
13:36	845	31.5	56.1	53.15	0.24	0.24
13:45	812	33	55.1	53.81	0.23	0.23

APPENDIX D

D.1 Thermal Performance of the Normal Inverter Air Conditioner Unit

Time	$T_{inlet,Eva}$ (°C)		$T_{outlet,Eva}$ (°C)		T_r (°C)	$T_{inlet,Cond}$ (°C)	$T_{outlet,Cond}$ (°C)	Q_{AC} (kW)	P_{AC} (kW)	SEER (kWh/kWh)
	<i>wb</i>	<i>db</i>	<i>wb</i>	<i>db</i>						
8:00	22.1	26	15.5	15.6	27.7	25.6	33.9	4.4	0.6	7.0
8:09	19.4	25.1	12.4	12.5	25	25.8	34.1	4.2	0.7	6.4
8:18	19.4	25	14.6	14.9	26.5	26.4	31.8	3.0	0.4	6.7
8:27	19.3	25.5	14.5	14.9	24.9	27.2	32.6	3.0	0.5	6.4
8:36	18.9	24.9	14.1	14.5	25.4	27.4	32.2	2.9	0.5	6.3
8:45	18.7	24.9	14	14.4	25.9	26.9	32.2	2.9	0.5	5.8
8:54	18.8	25.4	14.1	14.6	25.9	28.6	33.5	2.9	0.5	5.9
9:03	18.6	25.1	13.6	14	24.5	28.1	33.5	3.0	0.5	5.6
9:12	18.7	25.3	13.7	14.1	24.5	28.7	34.2	3.0	0.5	5.6
9:21	18.8	25.9	13.8	14.3	24.5	28.5	34	3.0	0.5	5.9
9:30	18.7	25.3	14	14.5	24.7	29.2	34.1	2.9	0.5	5.8
9:39	18.5	25.4	11.6	11.9	24.6	28.6	35.9	4.0	0.7	5.8
9:48	17.9	25.7	12.6	13.2	24.6	29.8	35.5	3.1	0.6	5.5
9:57	18.4	25.5	13.4	13.9	24.7	29	34.3	3.0	0.5	5.6
10:06	17.9	25.2	10.3	10.5	24.8	29.3	35.8	4.3	0.9	5.0
10:15	17.5	25.7	12.2	12.7	24.9	29	35	3.1	0.6	5.5
10:24	18.2	25.7	13.2	13.7	24.3	30	35.2	3.0	0.6	5.3
10:33	17.8	25.2	10.3	10.5	24.7	29.7	36.4	4.2	0.9	4.9
10:42	17.1	25.3	11	11.5	25	28.8	36.1	3.4	0.7	5.1
10:51	18	25.5	11.5	11.8	24.7	29.4	36.1	3.7	0.7	5.2
11:00	17.5	26.7	11	11.5	25.5	28.3	35.8	3.7	0.7	4.9
11:09	17.3	26.2	10.5	11.1	25.4	28.8	36.3	3.8	0.7	5.1
11:18	17.2	25.6	10.6	11	25.6	28.2	35.9	3.7	0.7	5.0

D.1 Thermal Performance of the Normal Inverter Air Conditioner Unit (continued)

Time	$T_{inlet,Eva}$ (°C)		$T_{outlet,Eva}$ (°C)		T_r (°C)	$T_{inlet,Cond}$ (°C)	$T_{outlet,Cond}$ (°C)	Q_{AC} (kW)	P_{AC} (kW)	SEER (kWh/kWh)
	wb	db	wb	db						
11:27	17.4	25.7	10.5	10.8	25.1	28.9	36.6	3.9	0.8	4.7
11:36	16.9	26.4	8.6	9	25.6	29.9	36.8	4.5	1.0	4.7
11:45	16.9	26.4	8.6	9	25.4	29.5	36.6	4.5	1.0	4.7
11:54	16.8	25.8	8.6	9	25.3	29.8	37	4.4	1.0	4.6
12:03	16.7	25.4	8.5	9	25.9	29.9	37	4.4	1.0	4.6
12:12	17	26.4	8.6	9.1	25.6	30.1	37	4.5	1.0	4.6
12:21	17	26.4	8.6	9	25.3	29.7	36.9	4.5	1.0	4.7
12:30	17.1	25.6	8.7	9.2	25.9	30	37.2	4.5	1.0	4.6
12:39	17.2	26.4	8.8	9.2	25.2	30.1	37.2	4.6	1.0	4.6
12:48	17.2	26.7	8.7	9.2	25	30.2	36.9	4.6	1.0	4.7
12:57	17	25.5	8.5	8.9	25.6	29.1	36.2	4.6	1.0	4.7
13:06	17.2	26.5	8.7	9.2	25.1	30	37.1	4.6	1.0	4.6
13:15	17.1	25.8	8.8	9.3	25.5	30.7	37.7	4.5	1.0	4.5
13:24	17.4	26.7	8.9	9.3	25.7	30	37.3	4.6	1.0	4.7
13:33	17.2	26.2	8.8	9.3	25.6	30.4	37.7	4.6	1.0	4.4
13:42	17.4	26.4	8.7	9.1	25.7	29.7	36.9	4.7	1.0	4.7
13:51	17.3	26.7	8.9	9.3	25.8	30.3	37.7	4.6	1.0	4.5
14:00	17.3	25.9	8.8	9.3	26	30.9	38	4.6	1.0	4.5
14:09	17.4	26.9	9	9.5	26.1	31.4	38.4	4.6	1.0	4.4
14:18	17.4	26	8.9	9.4	26.2	30.7	37.9	4.6	1.0	4.5
14:27	17.5	26.9	9	9.4	26.2	30.3	37.7	4.6	1.0	4.5
14:36	17.3	26.5	9	9.5	26.3	31.8	38.5	4.5	1.1	4.3
14:45	17.8	27	9.2	9.7	26.5	31.5	38.7	4.7	1.1	4.5
14:54	17.5	26.2	8.9	9.4	26.7	30.9	38.1	4.7	1.1	4.4
15:03	17.6	26.8	9.1	9.7	26.4	31.3	38.6	4.7	1.1	4.4
15:12	17.6	26.3	8.9	9.5	26.4	30.5	37.7	4.8	1.1	4.5
15:21	17.6	26.8	9	9.5	25.9	30.7	37.9	4.7	1.1	4.4
15:30	17.6	26.2	8.9	9.3	26	30.4	37.6	4.8	1.1	4.4
15:39	17.6	27	9	9.5	26	30.6	37.8	4.7	1.1	4.3
15:48	17.4	26	8.9	9.4	26.1	30.5	37.6	4.6	1.1	4.2

APPENDIX E

**Thermal Performance of the Inverter Air Conditioner Unit with PCM
Packed Bed.**

E.1 Electrical Power in Charging period at Various Thickness of PCM Bed

Time (min)	X=0.08m		X=0.16m		X=0.24m	
	Q_{AC} (kW)	P_{AC} (kW)	Q_{AC} (kW)	P_{AC} (kW)	Q_{AC} (kW)	P_{AC} (kW)
1	0.00	0.00	0.00	0.00	0.00	0.00
5	1.60	0.43	1.65	0.50	1.75	0.36
9	1.43	0.38	1.60	0.40	1.70	0.55
13	1.25	0.28	1.25	0.34	1.55	0.34
17	0.98	0.23	1.17	0.24	1.47	0.24
21	0.90	0.23	1.01	0.20	1.21	0.20
25	0.90	0.23	0.85	0.17	1.15	0.17
29	0.86	0.23	0.85	0.20	1.15	0.20
33	0.88	0.23	0.77	0.15	0.97	0.15
37	0.87	0.23	0.59	0.15	0.79	0.15
41	0.88	0.23	0.42	0.15	0.62	0.15
45	0.85	0.23	0.74	0.20	0.94	0.20
49	0.60	0.23	0.78	0.20	0.98	0.20
53	0.53	0.23	0.70	0.20	0.90	0.20
57	0.45	0.23	0.51	0.17	0.71	0.17
61	0.44	0.24	0.67	0.17	0.67	0.17
65	0.60	0.17	0.78	0.22	0.98	0.22
69	0.20	0.17	0.69	0.15	0.89	0.15
73	0.40	0.19	0.66	0.15	0.86	0.15
77	0.31	0.19	0.50	0.21	0.70	0.21
81	0.25	0.19	0.36	0.17	0.56	0.17
85	0.20	0.19	0.20	0.15	0.40	0.15
89	0.19	0.19	0.48	0.14	0.68	0.14
93			0.50	0.17	0.70	0.17
97			0.47	0.17	0.67	0.17
101			0.42	0.17	0.62	0.17

E.1 Electrical Power in Charging period at Various Thickness of PCM Bed (continued)

Time (min)	X=0.08m		X=0.16m		X=0.24m	
	Q_{AC} (kW)	P_{AC} (kW)	Q_{AC} (kW)	P_{AC} (kW)	Q_{AC} (kW)	P_{AC} (kW)
105			0.37	0.17	0.57	0.17
109			0.74	0.29	0.94	0.29
113			0.52	0.22	0.72	0.22
117			0.49	0.22	0.69	0.22
121			0.51	0.22	0.71	0.22
125			0.36	0.17	0.56	0.17
129			0.33	0.17	0.53	0.17
133			0.31	0.17	0.51	0.17
137			0.29	0.17	0.49	0.17
141			0.29	0.17	0.49	0.17
145			0.29	0.17	0.49	0.17
149			0.26	0.17	0.46	0.17
153					0.75	0.33
157					0.61	0.21
161					0.61	0.21
165					0.57	0.21
169					0.32	0.17
173					0.23	0.15
177					0.23	0.12
181					0.32	0.19
185					0.34	0.17
189					0.34	0.17

ลิขสิทธิ์มหาวิทยาลัยเชียงใหม่
Copyright © by Chiang Mai University
All rights reserved

E.2 Electrical Power in Discharging period at Various Thickness of PCM Bed

Time (min)	X=0.08m		X=0.16m		X=0.24m	
	Q_{AC} (kW)	P_{AC} (kW)	Q_{AC} (kW)	P_{AC} (kW)	Q_{AC} (kW)	P_{AC} (kW)
1	0.08	0.23	0.04	0.23	0.00	0.54
10	1.77	0.37	1.94	0.32	2.07	0.30
19	1.34	0.31	1.35	0.24	1.32	0.23
28	1.09	0.28	0.99	0.19	1.05	0.20
37	1.10	0.28	1.80	0.34	1.07	0.22
46	1.81	0.28	1.02	0.15	0.41	0.31
55	1.43	0.28	1.61	0.22	0.41	0.20
64	1.14	0.28	1.05	0.24	0.82	0.20
73	1.83	0.31	1.46	0.31	0.45	0.21
82	1.63	0.31	1.15	0.24	1.08	0.23
91	1.64	0.42	1.69	0.22	0.82	0.23
100	1.97	0.33	1.22	0.34	1.28	0.20
109	2.05	0.37	1.71	0.36	0.97	0.25
118	1.50	0.33	1.74	0.33	1.49	0.20
127	2.01	0.38	1.88	0.33	1.50	0.22
136	2.08	0.40	1.79	0.31	1.56	0.25
145	2.08	0.44	1.90	0.31	1.65	0.25
154	2.20	0.37	1.82	0.30	1.65	0.23
163	2.13	0.38	1.90	0.31	1.66	0.30
172	2.02	0.40	1.84	0.31	1.64	0.25
181	2.09	0.43	1.87	0.31	1.52	0.27
190	2.14	0.64	1.78	0.57	1.61	0.50
199	2.12	0.43	1.76	0.58	1.61	0.55
208	2.17	0.66	2.44	0.58	1.57	0.55
217	2.19	0.47	2.61	0.49	1.72	0.55
226	2.23	0.66	2.69	0.34	1.67	0.58
235	2.23	0.66	2.24	0.60	2.43	0.44
244	2.94	0.66	2.09	0.62	2.04	0.58
253	2.34	0.66	2.87	0.62	2.04	0.39
262	2.82	0.57	2.97	0.62	2.62	0.55
271	2.67	0.76	2.98	0.62	2.29	0.39

E.2 Electrical Power in Discharging period at Various Thickness of PCM Bed
(continued)

Time (min)	X=0.08m		X=0.16m		X=0.24m	
	Q_{AC} (kW)	P_{AC} (kW)	Q_{AC} (kW)	P_{AC} (kW)	Q_{AC} (kW)	P_{AC} (kW)
280	3.04	0.76	3.00	0.62	2.77	0.58
289	2.93	0.75	3.00	0.64	2.77	0.58
298	2.95	0.75	3.06	0.64	2.83	0.57
307	2.95	0.75	3.03	0.61	2.77	0.57
316	2.48	0.78	3.03	0.71	2.80	0.57
325	3.11	0.78	3.05	0.74	2.75	0.57
334	3.07	0.78	3.11	0.74	2.78	0.58
343	3.18	0.78	3.07	0.74	2.77	0.58
352	3.19	0.75	3.11	0.74	2.89	0.58
361	3.23	0.75	3.07	0.74	2.77	0.60
370	3.31	0.75	3.11	0.74	2.99	0.58
379	3.25	0.75	3.07	0.74	2.98	0.58
388	3.18	0.76	3.14	0.73	3.11	0.58
397	3.27	0.76	3.09	0.73	3.08	0.73
406	3.29	0.76	3.11	0.73	3.00	0.73
415	3.18	0.76	3.14	0.75	3.20	0.73
424	3.24	0.76	3.19	0.75	3.15	0.75
433	3.36	0.75	3.16	0.75	3.25	0.73
442	3.34	0.76	3.24	0.75	3.20	0.73
451	3.28	0.76	3.41	0.75	3.32	0.73
460	3.05	0.76	3.31	0.75	3.18	0.73
469	3.30	0.76	3.47	0.75	3.26	0.73
478	3.22	0.76	3.31	0.78	3.13	0.73
481	3.33	0.76	3.09	0.75	3.00	0.73

CURRICULUM VITAE

Author's Name	Mr. Songheng Loem
Date/Year of Birth	06 th April 1993
Place of Birth	Kampong Thom
Education	2019- Master's Degree, Faculty of Engineering, Chiang Mai University, Thailand 2017 Bachelor's Degree, Faculty of Mechanical and Industrial Engineering, Institute of Technology of Cambodia, Cambodia 2012 High School Diploma, Triel High School, Cambodia
Scholarship	2-year Scholarship, Faculty of Engineering, Chiang Mai University under Research Assistant Program
Publications	Songheng Loem and Thoranis Deethayat, "Optimum Number of Solar Cell Modules with And Without Phase Change Material Cooling for Air-Conditioning" The 17 th Conference on Energy, Heat and Mass Transfer in Thermal Equipment and Processes, Lampang Resort, Thailand. 15-16 February 2018 Songheng Loem, Thoranis Deethayat, Attakorn Asanakham and Tanongkiat Kiatsiroat, "Thermal characteristics on melting/solidification of low temperature PCM balls packed bed with air charging/discharging". Case Stud. Therm. Eng., vol. 14, p. 100431, Mar. 2019.

